Memorandum of Understanding 19071/05/NL/CP

UNIVERSITEIT GENT

FACULTEIT WETENSCHAPPEN

MELiSSA FOOD CHARACTERIZATION: PHASE 1

TECHNICAL NOTE: 98.8.3

DESIGN OF A PLANT CHARACTERIZATION UNIT: STUDY OF CRITICAL SUBSYSTEMS AND SELECTION OF MOST SUITABLE TECHNOLOGIES

prepared by/*préparé par*	Matteo Nobili, Lorenzo Bucchieri, Chloe Girard, Michael Stasiak
reference/*réference*	Contract number 22070/08/NL/JC
issue/*édition*	1
revision/*révision*	0
date of issue/*date d'édition*	28.01.2011
status/*état*	Final
Document type/*type de document*	Technical Note
Distribution/*distribution*	FC1 consortium, ESA/ESTEC

CONFIDENTIAL DOCUMENT

APPROVAL

Title *titre*	Design of a plant characterization unit: Study of critical subsystems and selection of most suitable technologies	Issue *issue*	1	revision 0 *revision*

Author *auteur*	Chloe Girard, Matteo Nobili, Lorenzo Bucchieri, Michael Stasiak, Mike Dixon	date *date*	28.01.201

Reviewed by (UGent)	Martin Weihreter	date *date*	16.12.2010
approved by (UGent) *approuvé by*	Dominique Van Der Straeten		23.12.2010

CHANGE LOG

reason for change /*raison du changement*	issue/*issue*	revision/*revision*	date/*date*
Submission to ESA/ESTEC	1	0	23.12.2010

CHANGE RECORD

Issue: 1 Revision: 0

reason for change/*raison du changement*	page(s)/*page(s)*	paragraph(s)/*paragraph(s)*

Table Of Contents

Table of Figures

List of Tables

List of Abbreviations

CFD:	Computational Fluid Dynamics
FC:	Food Characterization (project)
HVAC:	Heating, Ventilation and Air Conditioning
PCU:	Plant Characterization Unit
PSA:	Pressure Swing Adsorption
WP:	Work Package

1 Introduction

Over the last year, the Food Characterization (FC) group of scientists have conducted ground based experiments on wheat, soybean, and potato grown under controlled conditions, not only to produce crop productivity data, but to give an insight into problems that may arise during the growing process. The purpose of present and future ground based experimentation is the generation of repeated and statistically reproducible crop growth characterisation data for use in modelling, and to ultimately provide hardware and sensor specifications that will produce a reliable and predictable closed regenerative support system. To that end, the design of the ground based plant characterisation unit (PCU) must meet the rigours of daily operation over long periods of time with reliability and stable performance.

This technical note focuses on the critical subsystem components and criteria that have a perceived need for further study to improve system operation and reliability. Over the course of the ground experiments and PCU design iterations, a number of critical issues have arisen and include:

- air homogeneity
- oxygen removal
- ethylene mitigation

The following documents current information and identifies possible methods of mitigating these issues.

2 Air Handling

A preliminary design of the PCU air distribution system accounting for building and maintenance constraints is proposed. The suggested design is analysed via CFD simulation to test the fluid dynamic performance and fine tune the simulation set up.

Contour plot of pressure and velocity fields are analysed and numerical convergence of the solution assessed.

The model was developed using ICEM-HEXA (automatic mesh generation) and ANSYS CFX (CFD solution).

2.1 Preliminary design

The main purposes of the preliminary design were to:

- Establish the overall dimensions of the system
- Verify that all the constraints are fulfilled.
- Obtain a clear picture of the system and of its flow field
- Use the result to determine the critical areas for a final optimized design

The type and the specifics of the devices used to move and condition air were selected by UoGuelph and were actually part of the constraints of the air handling system (TN 98.8.1). The elements used to distribute and balance the flow were designed by Enginsoft and approved by UGent.

Geometry and computational grid

The air handling system (Fig. 1) is comprised of two compartments referred to as 'HVAC' and 'Air distribution'. The HVAC compartment is the volume located behind the growth chamber where the heat exchangers and the blower are positioned. The air distribution compartment is the volume right below the growth chamber where the air pressurized by the blower is conveyed. The two compartments and the growth chamber are connected in a closed loop.

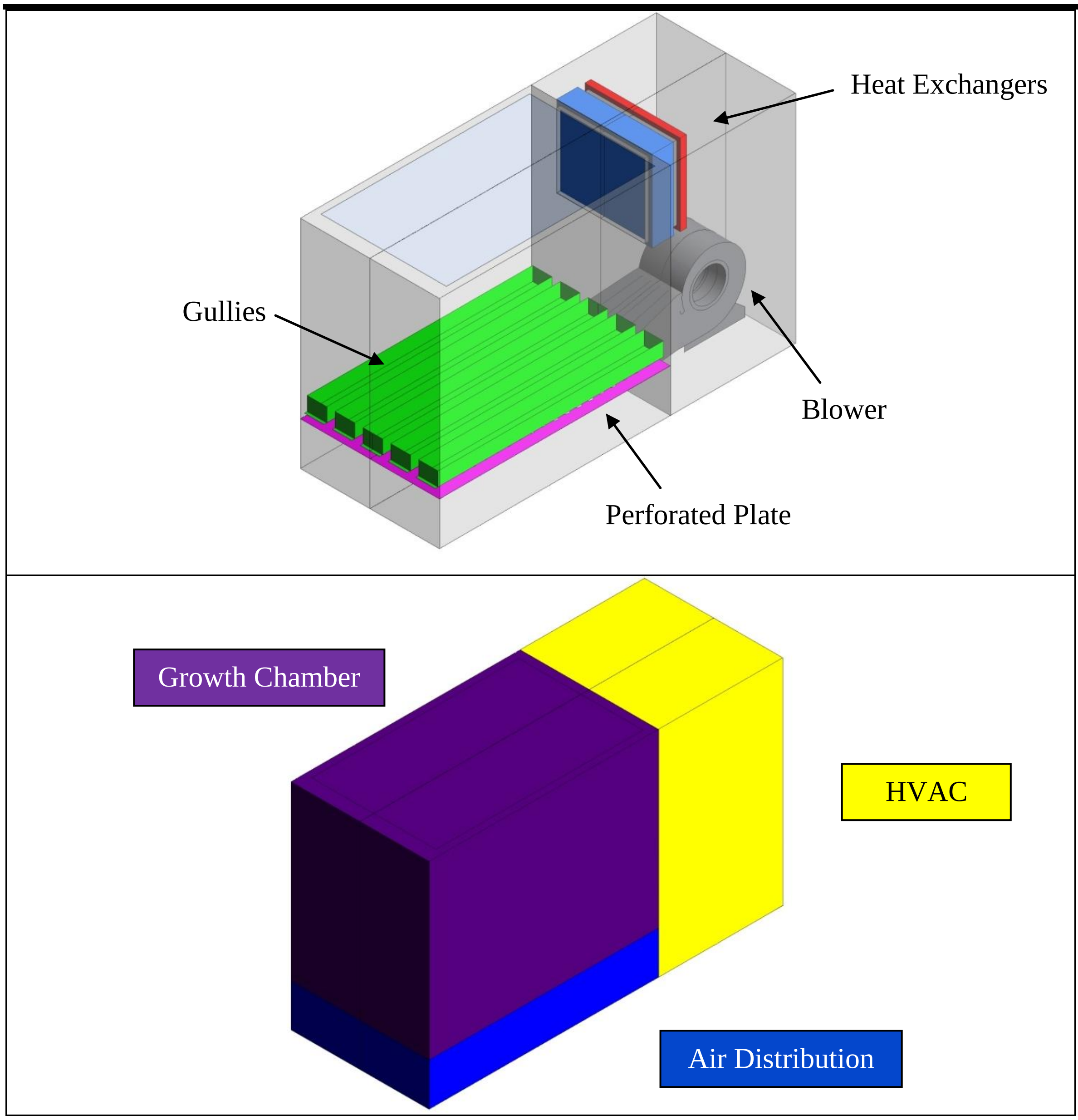

Fig. 1 Air handling system partitioning

Fig. 2 and Fig. 3 show schematics of the air handling system arrangement. The general dimensions as well as the location of the devices are clearly highlighted. The maximum admissible depth of the HVAC (90cm) was used and the air outlet of the growth chamber was horizontally centred and positioned 5cm from the top.

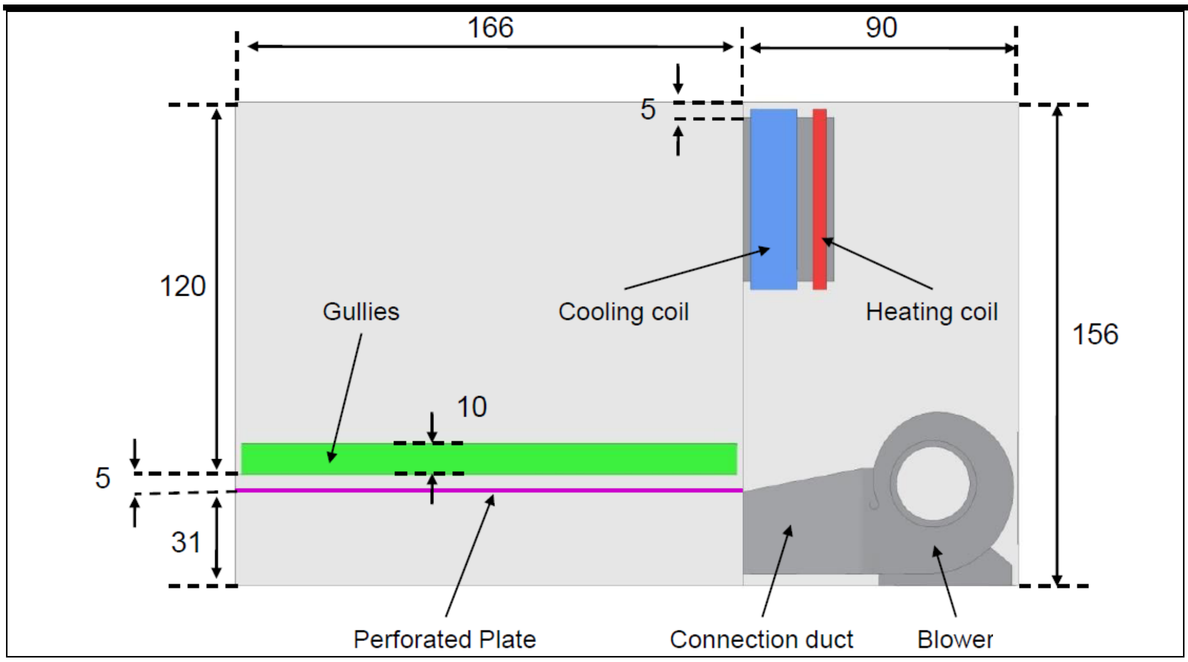

Fig. 2 Schematic of the air handling system arrangement: lateral view (units: cm)

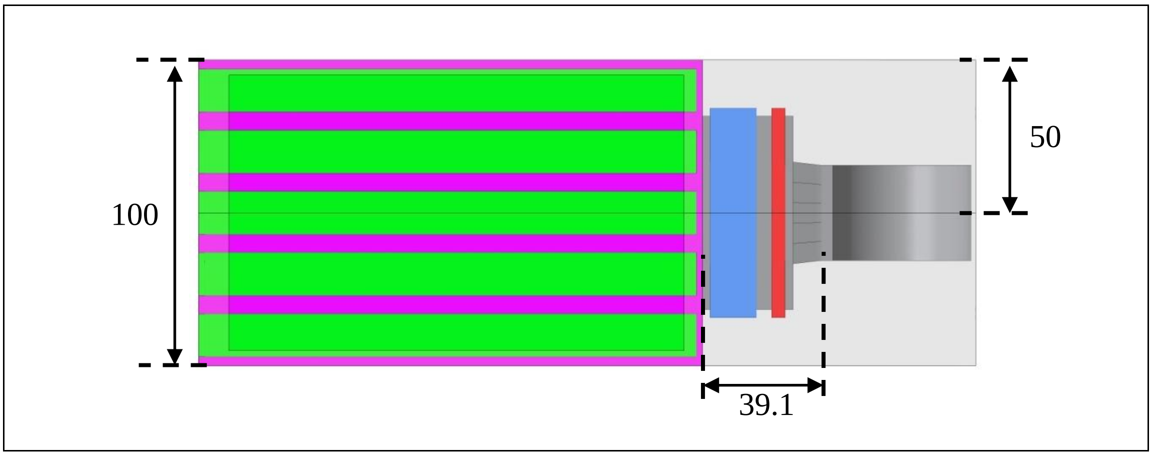

Fig. 3 Schematic of the air handling system arrangement: top view (units: cm)

In order to promote a uniform air distribution in the growing chamber, Enginsoft proposed the following technical solutions:

- Interpose a perforated plate between the air distribution compartment and the growth chamber.
- Connect the HVAC compartment and the air distribution compartment by means of a baffled duct.

The layout of the perforated plate is shown in Fig. 4. It consists of five columns of holes (one under each gully) each made by nineteen rows. The diameters of the holes are reported in the table below:

01	**02**	**03**	**04**	**05**	**06**	**07**	**08**	**09**	**10**	**11**	**12**	**13**	**14**	**15**	**16**	**17**	**18**	**19**	
2.0	*2.0*	*2.5*	*2.5*	*3.0*	*3.0*	*3.0*	*3.0*	*3.5*	*3.5*	*4.0*	*4.0*	*4.5*	*4.5*	*5.0*	*5.0*	*5.5*	*5.5*	*6.0*	**cm**

Tab. 1 Hole diameters

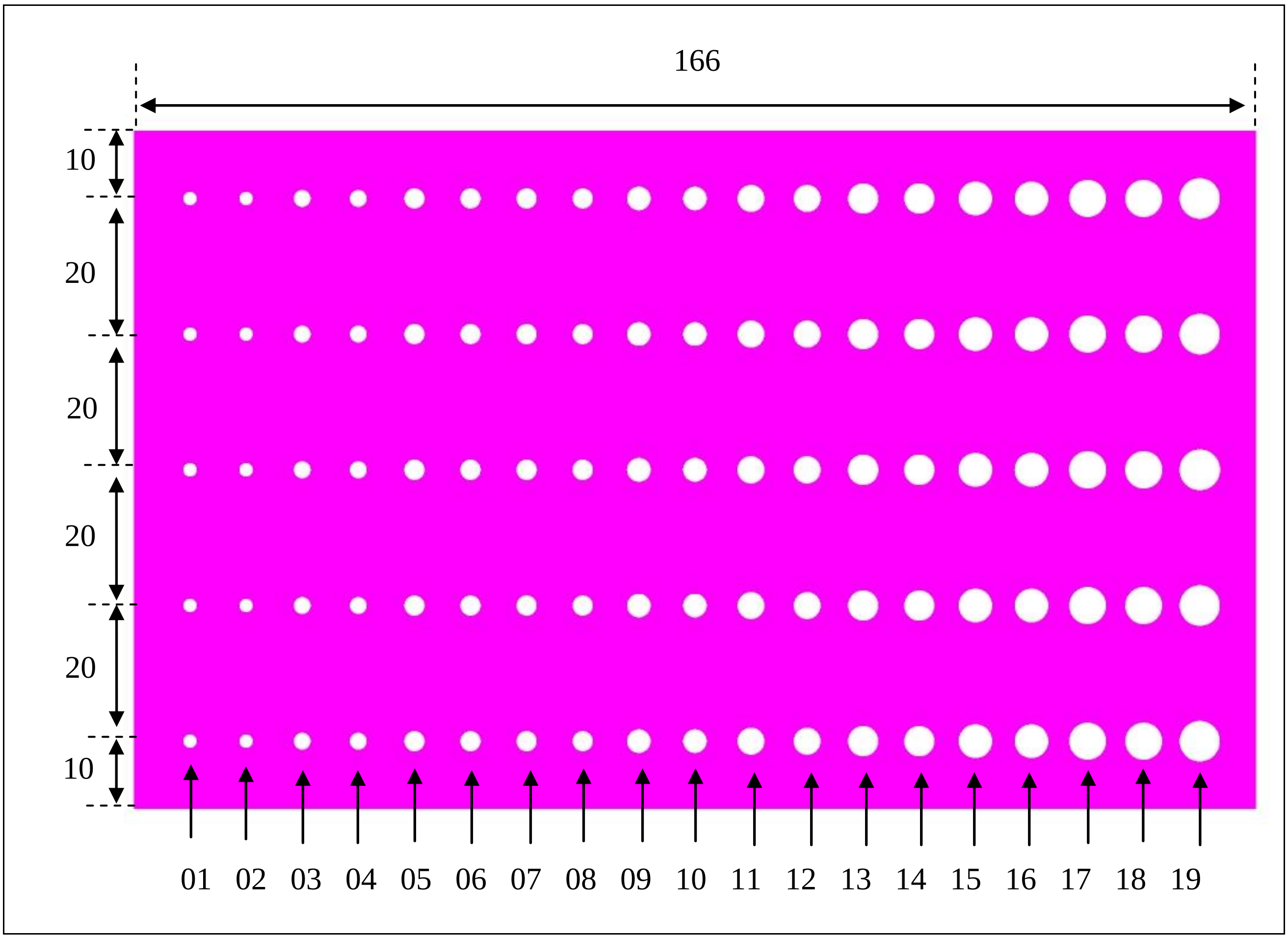

Fig. 4 Perforated plate (units: cm)

Two main objectives guided the design of the perforated plate:

- Avoid flow recirculation though the holes
- Reduce the strength of the jet flows plants are exposed to

This document is confidential property of the MELiSSA partners and shall not be used, duplicated, modified or transmitted without their authorization
Memorandum of Understanding 19071/05/NL/CP

The first objective was achieved by keeping the dimension of the holes small (max diameter 6cm) and by employing a relatively large number of rows (19).

The second objective was solved by locating the perforated plate 5cm below the gullies (as shown in Fig. 2) and by placing each column on the midline position of the matching gully. This way the bottom surface of the gullies provide an impingement surface to the air flow which prevents plants from being directly exposed to the jet flows.

The geometry of the connection duct and its dimensions are shown in Fig. 5. The cross sectional area of the duct is kept constant over its length to prevent sudden changes in air velocity. Moreover four equally spaced baffles are placed inside the duct to avoid localized pressure drops due to the detachment of the fluid vein.

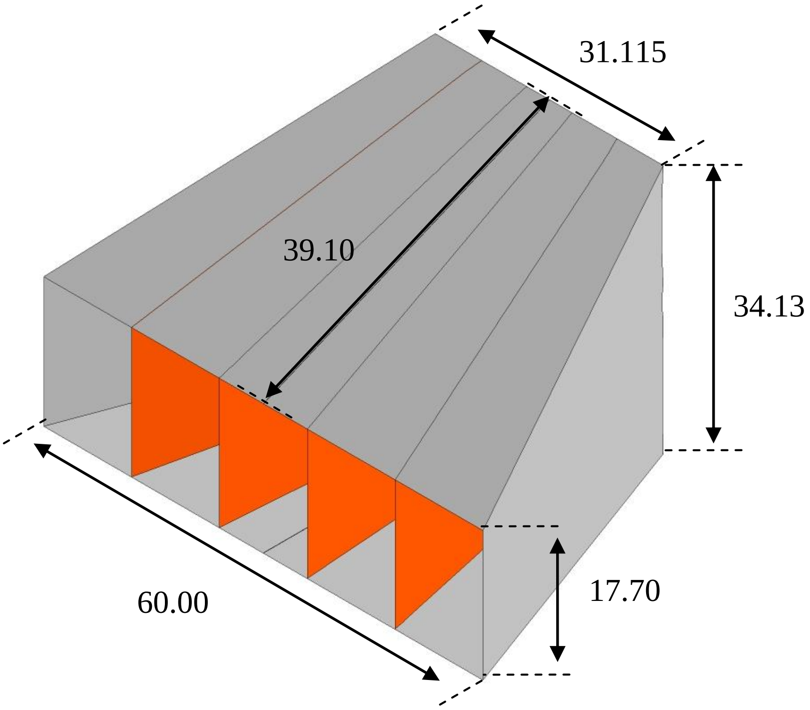

Fig. 5 Connection duct (units: cm)

The Grids of the computational domain were generated with the HEXA module of the meshing code ANSYS ICEM. The following table resumes the mesh features for each compartment:

	Number of Elements	**Minimum Angle**	**Aspect Ratio**
HVAC	179858	17.7	47
Air Distribution	644722	20.7	104
Growth chamber	1289444	75	201
Totals	2114024		

Tab. 2 Mesh features

See below for some details of the mesh.

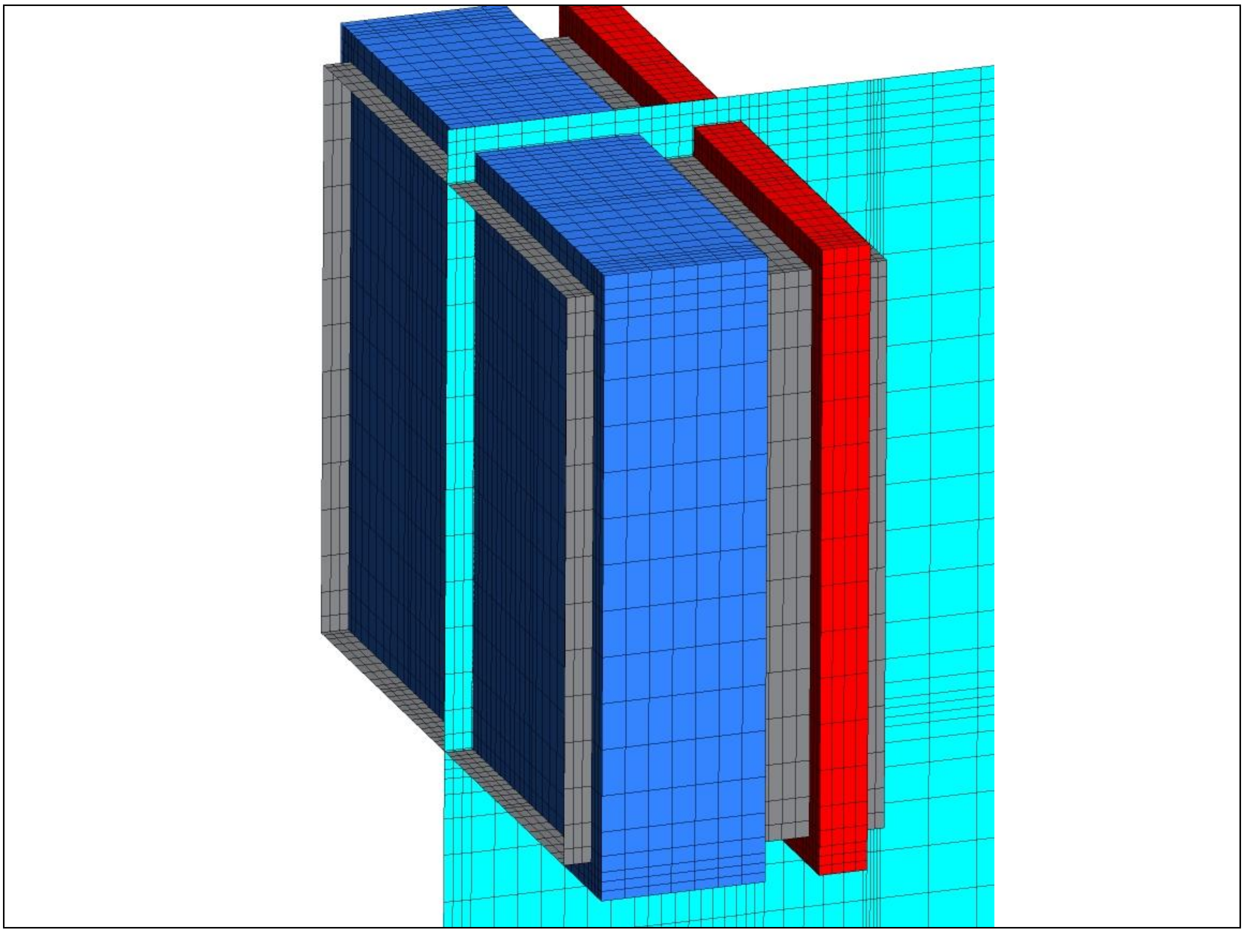

Fig. 6 HVAC mesh: heat exchangers

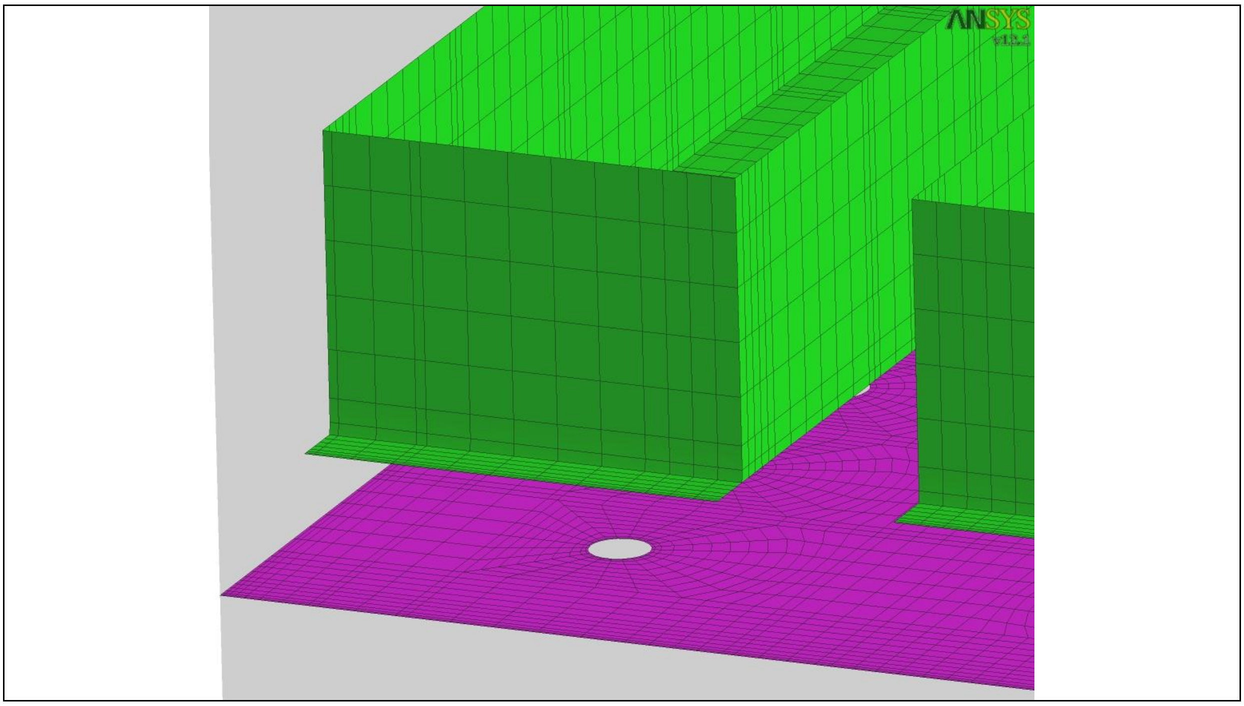

Fig. 7 Growth chamber gullies and perforated plate

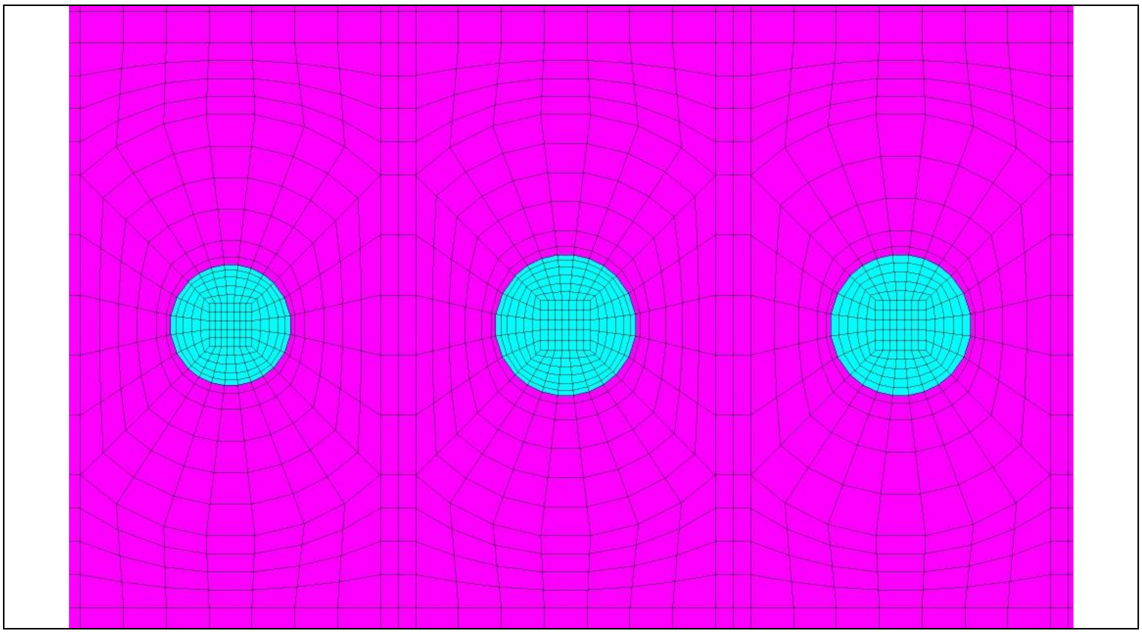

Fig. 8 Air distribution compartment: perforated plate and holes

This document is confidential property of the MELiSSA partners and shall not be used, duplicated, modified or transmitted without their authorization
Memorandum of Understanding 19071/05/NL/CP

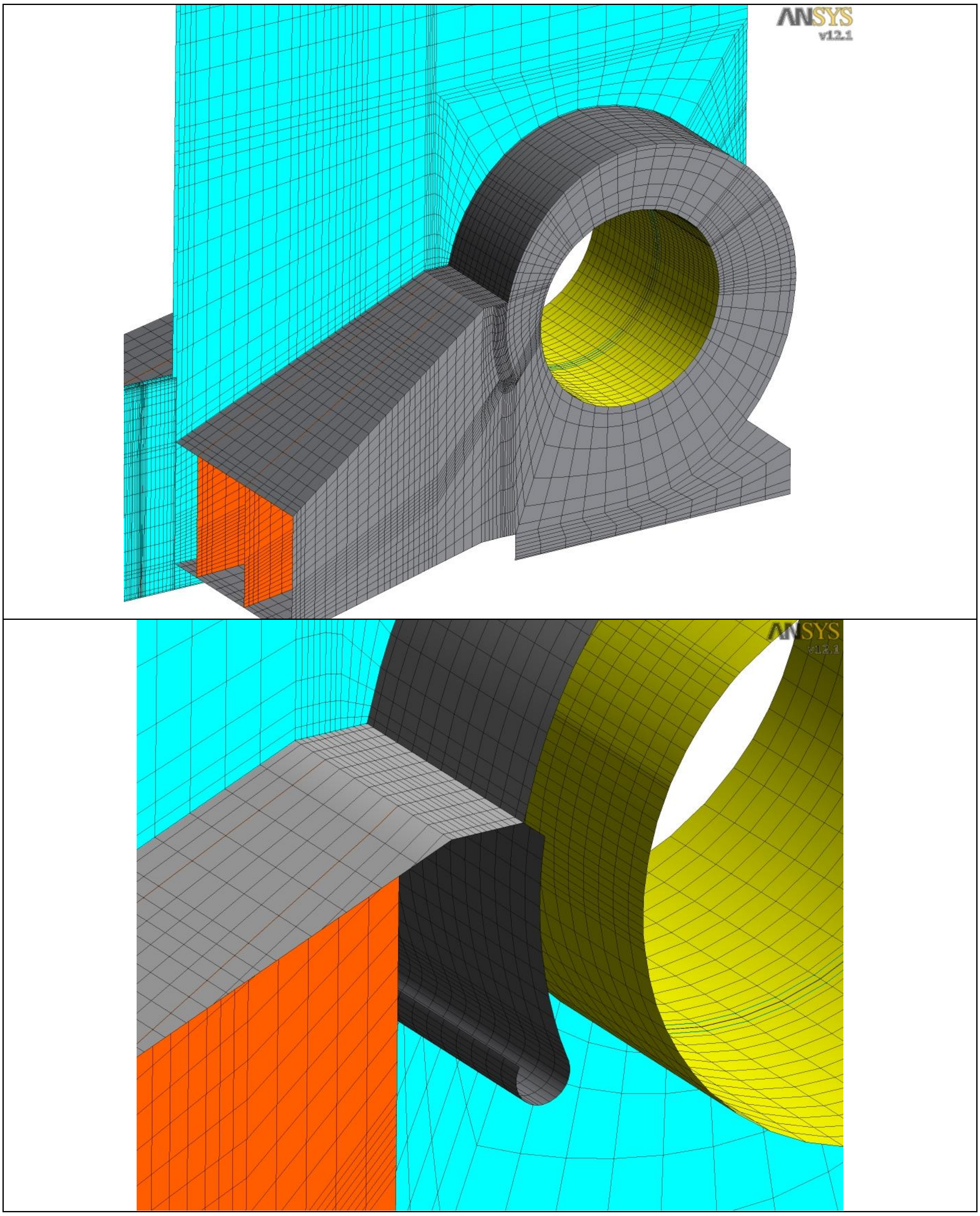

Fig. 9 HVAC mesh: blower region

Physical properties and boundary conditions

The PCU is supposed to be in stable thermal condition at 21.5°C and the energy equation is not solved.

A **symmetry** boundary condition has been placed on the middle plane of the PCU model since the geometry and the expected flow patterns are identical on either side of the dividing plane. This assumption reduces by half the computational costs.

All the **internal and external walls** of the domain are treated as smooth with a no slip condition applied.

Since the aim of the study is to evaluate and optimise the global performances of the system and not to analyse in detail each single element, the explicit modelling of the **blower** is out of scope. Moreover the explicit introduction of this element would have required significant geometrical complications and a considerable mesh refinement. Hence its influence on the global fluid dynamic behaviour has been modelled by introducing equivalent 3D sub domains where momentum source is applied.

The momentum source has the following expression:

$$\frac{\partial P}{\partial x} = C1 + C2 \cdot |Q| + C3 \cdot |Q|^2 \qquad [1]$$

where Q is mass flow through the blower

This source reproduces the real characteristic curve of the air movement equipment. This way the response of the blower to any change of the resistance imposed to the air flow (system curve) is directly taken into account without explicitly modelling it.

The value of the coefficients in equation [1] have been estimated from the Med (motor speed) characteristic curve provided by UGent [ref1] which is shown in the figure below. This curve represents the performance of the blower at a medium motor speed.

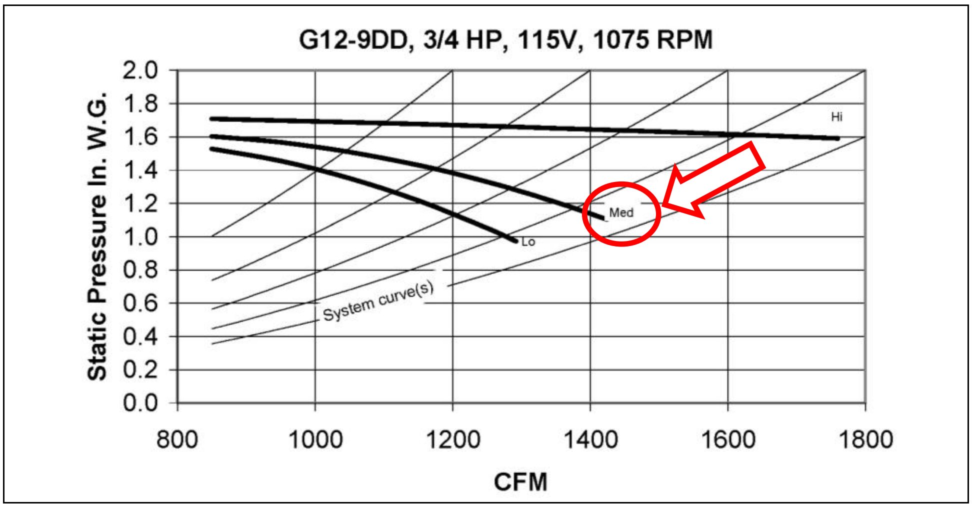

Fig. 10 Blower performance curve

Tab. 3 shows the values of the three coefficients for the Med curve reported in Fig. 10.

Coefficient	Value
C1 [Kg m^{-2} s^{-2}]	4584.8
C2 [m^{-2} s^{-1}]	19767
C3 [Kg^{-1} m^{-2}]	-50071

Tab. 3 Coefficient for the momentum source

For the same reasons as mentioned for the blower, the **water coils** (cooler and heater) are modelled by the addition of a momentum sink in the governing momentum equations. The momentum loss in the stream wise direction is calculated as:

$$\frac{\partial p}{\partial x_i} = -D1 \cdot U_i - D2 \cdot |U_i|^2 \qquad [2]$$

where *D1* is the linear loss coefficient, *D2* is the quadratic loss coefficient, U_i is the local velocity in the stream wise direction and $\partial p / \partial x_i$ is the pressure drop gradient in the stream wise direction.

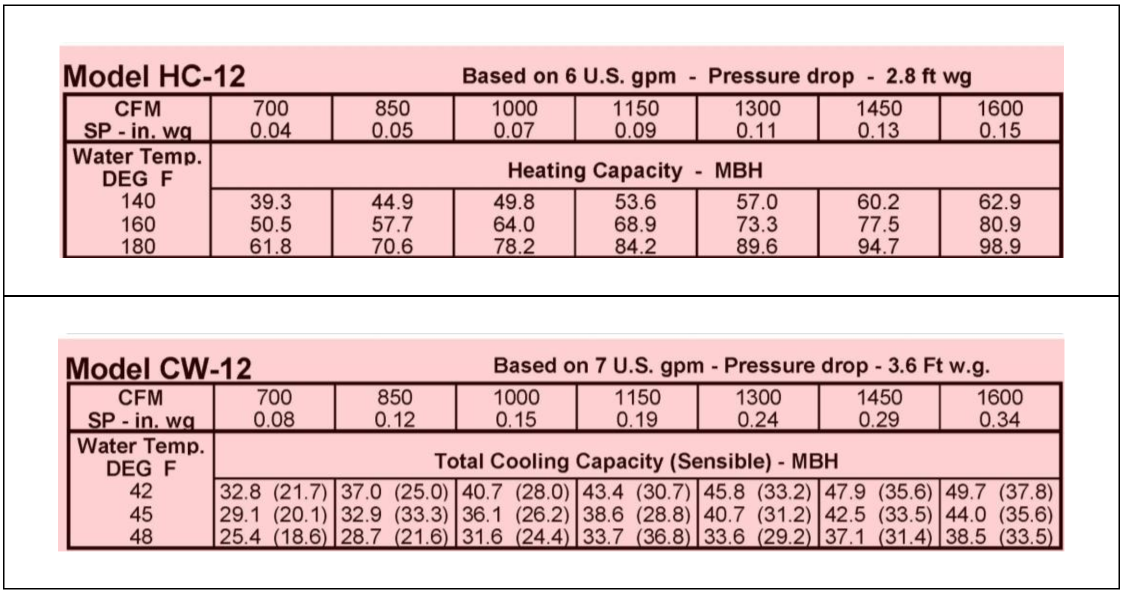

Model HC-12 Based on 6 U.S. gpm - Pressure drop - 2.8 ft wg

CFM SP - in. wg	700 0.04	850 0.05	1000 0.07	1150 0.09	1300 0.11	1450 0.13	1600 0.15
Water Temp. DEG F	Heating Capacity - MBH						
140	39.3	44.9	49.8	53.6	57.0	60.2	62.9
160	50.5	57.7	64.0	68.9	73.3	77.5	80.9
180	61.8	70.6	78.2	84.2	89.6	94.7	98.9

Model CW-12 Based on 7 U.S. gpm - Pressure drop - 3.6 Ft w.g.

CFM SP - in. wg	700 0.08	850 0.12	1000 0.15	1150 0.19	1300 0.24	1450 0.29	1600 0.34
Water Temp. DEG F	Total Cooling Capacity (Sensible) - MBH						
42	32.8 (21.7)	37.0 (25.0)	40.7 (28.0)	43.4 (30.7)	45.8 (33.2)	47.9 (35.6)	49.7 (37.8)
45	29.1 (20.1)	32.9 (33.3)	36.1 (26.2)	38.6 (28.8)	40.7 (31.2)	42.5 (33.5)	44.0 (35.6)
48	25.4 (18.6)	28.7 (21.6)	31.6 (24.4)	33.7 (36.8)	33.6 (29.2)	37.1 (31.4)	38.5 (33.5)

Fig. 11 Heating and cooling coils experimental data

Experimental data available from the manufacturer in the form of pressure drop against mass flow through the air conditioning devices were used to determine the value of the linear and quadratic loss coefficients of equation [2].

Tab. 4 reports the calculated values.

Coefficient	Cooling	Heating
D1 [Kg^{-1} m^{-2}]	77.142	109.07
D2 [Kg m^{-4}]	122.47	121.15

Tab. 4 Coefficients for the momentum sinks

The influence of the **plants** on the air flow has been taken into account by applying a localized pressure gradient to the 3D porous region which schematically represents the plant itself. As shown in Fig. 12 the 3D porous region is located at the top of the gullies and has the following dimensions:

Depth	100[cm]	Depth of the chamber
Height	90[cm]	Leaf level has defined in TN 98.7 [ref 3]

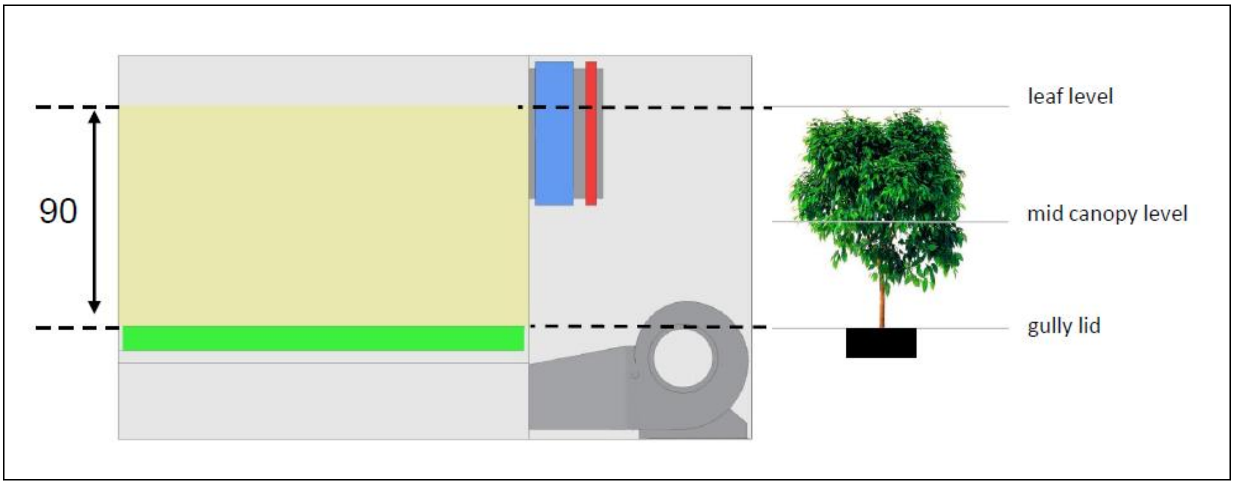

Fig. 12 Plant modelling

An isotropic pressure loss with loss coefficient of $50[m^{-1}]$ is applied. The value of the coefficient is an educated guess since no experimental data is available.

Numerical procedure

The analyses of the three domains have been set up following the same numerical:

- Analysis type
    - Steady state
- Advection Scheme
    - High Resolution (2nd order accurate)
- Turbulence Numeric
    - First Order
- Fluid False Timescale Control
    - Time scale control: Local Timescale
    - Length scale option: Conservative
    - Timescale factor: 1.0
- Convergence Criteria:
    - Residual Target: 1.0E-6

This set up method is a good compromise between result quality and analysis speed, without interfering with its robustness.

Results

The aim of this preliminary analysis is to determine the flow rate, to assess the circulation of the airflow in the chamber and to work out the pressure and velocity distribution in the air handling system compartments.

The results of this analysis will be the reference point for the subsequent parametric study detailed in TN 98.8.4.

In the figure below the blower characteristic curve and its working point are shown.

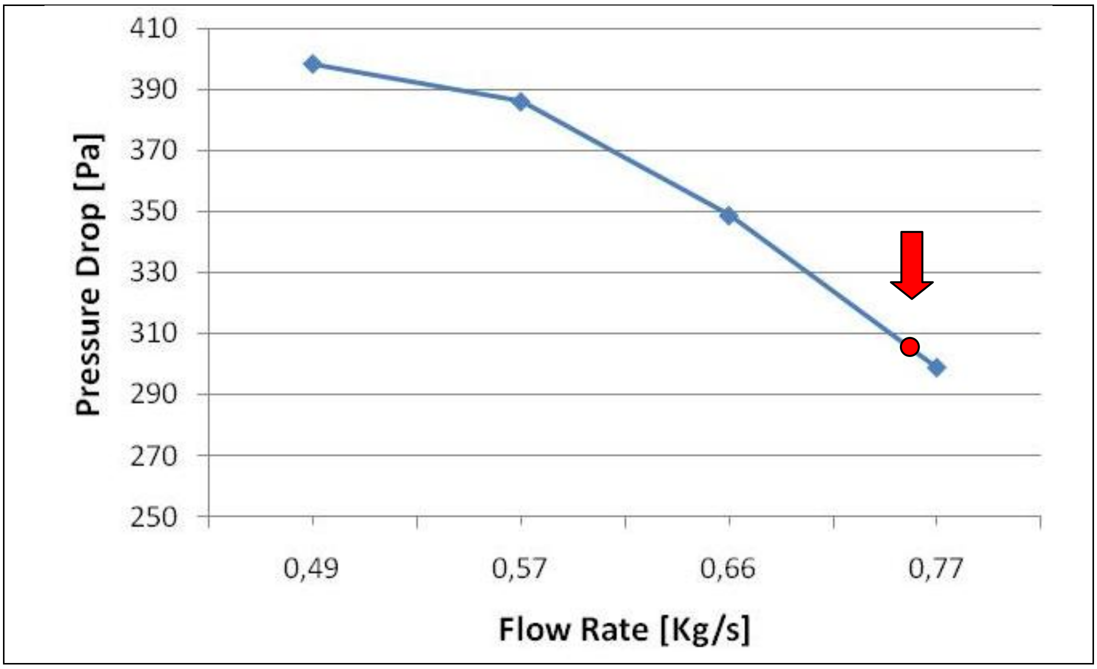

Fig. 13 Blower curve and working point for a medium motor speed

The calculated flow rate (0.74 [kg s^{-1}] equal to 37141.27 [l min^{-1}]) at medium blower speed is in the range of the expected performance estimated for two extreme air velocity scenarios in the growing chamber (minimum 8964 [l min^{-1}] and maximum 43824 [l min^{-1}]) [paragraph 3.3.1, TN 98.8.1]. This confirms the preliminary hardware choice to reach the specifications described in TN 98.8.1 with respect to air velocity.

HVAC compartment

Fig. 14 and Fig. 15 show the pressure and velocity contours inside the HVAC compartment on different planes. The pressure drop in the water coils is clearly visible as well as the action of the blower.

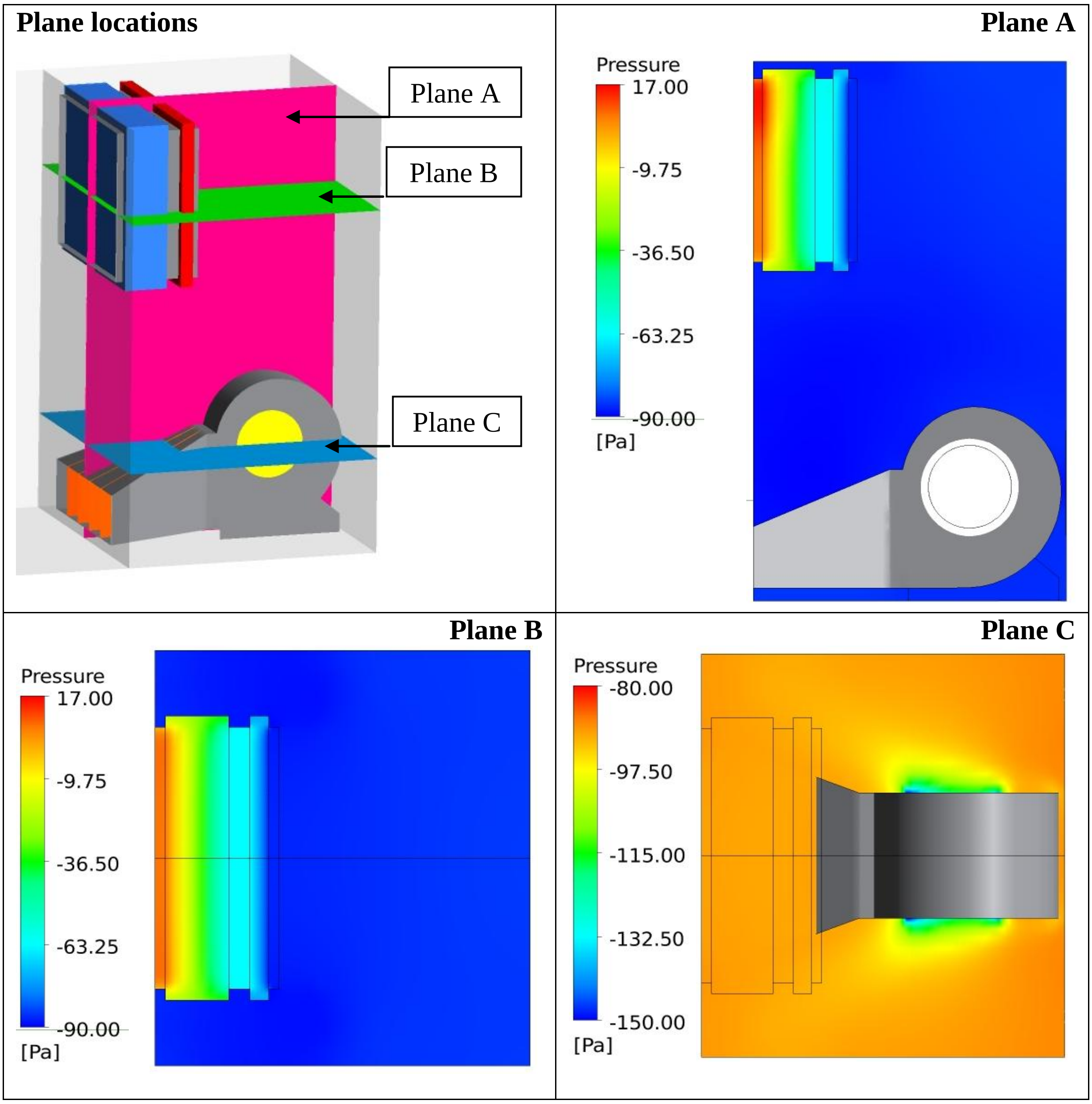

Fig. 14 HVAC compartment: static pressure contours

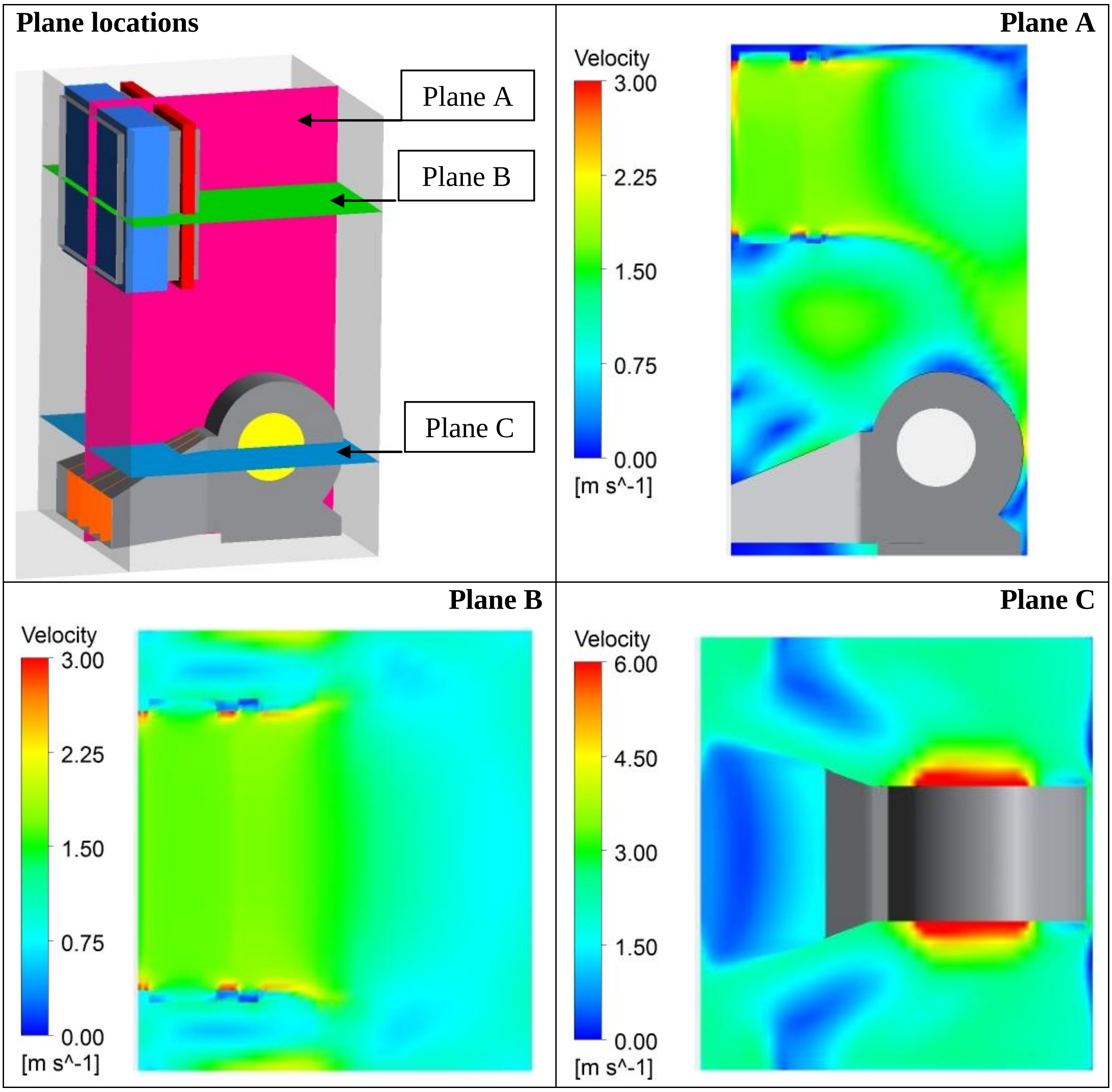

Fig. 15 HVAC compartment: velocity contours

Fig. 16 displays the streamlines coloured by velocity. This figure demonstrates how the position of the blower shifted along the longitudinal plane with respect to the heating coils allows the flow to gently turn when moving from the top to the bottom of the HVAC compartment. Recirculation regions are located at the sides of the water coils and in proximity of the blower.

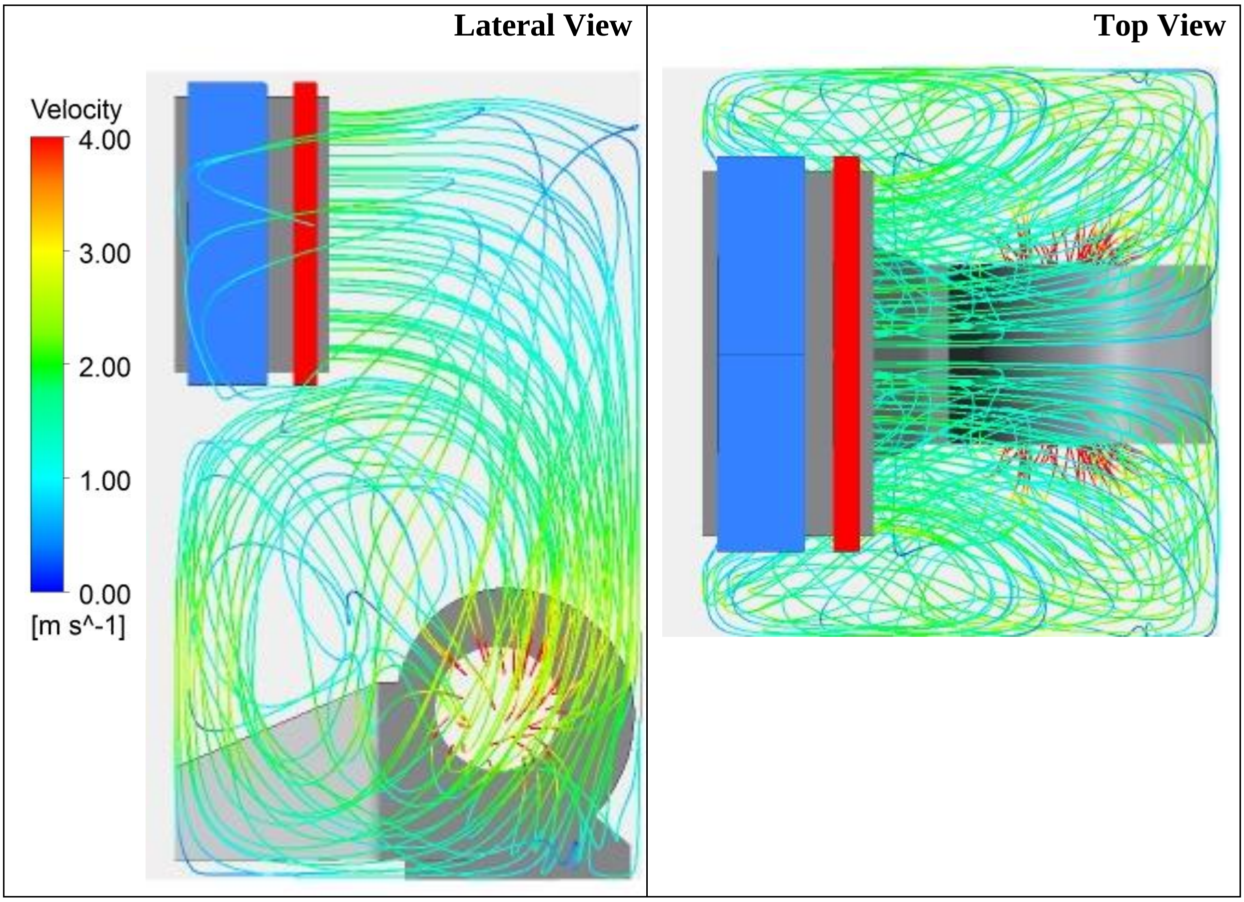

Fig. 16 HVAC compartment: streamlines

Air distribution compartment

Fig. 17, Fig. 18 and Fig. 19 illustrate the details of the flow field in the air compartment. It's evident that:

- A strong pressure gradient is present between front and back regions
- Higher pressure values can be found at the front of the compartment
- Recirculation areas can be noticed at the exit of the connection duct and at the front of the compartment

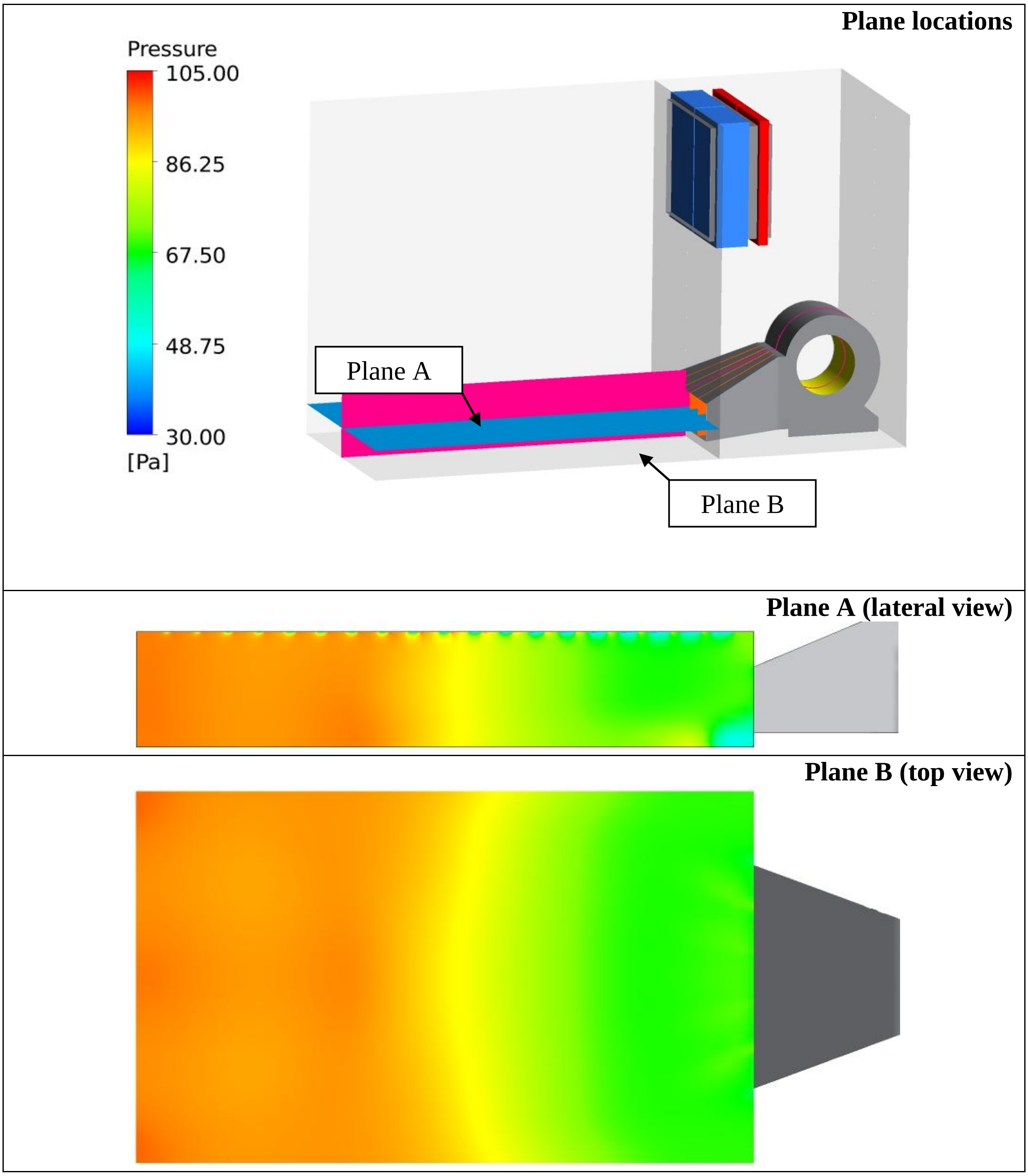

Fig. 17 Air compartment: static pressure contours

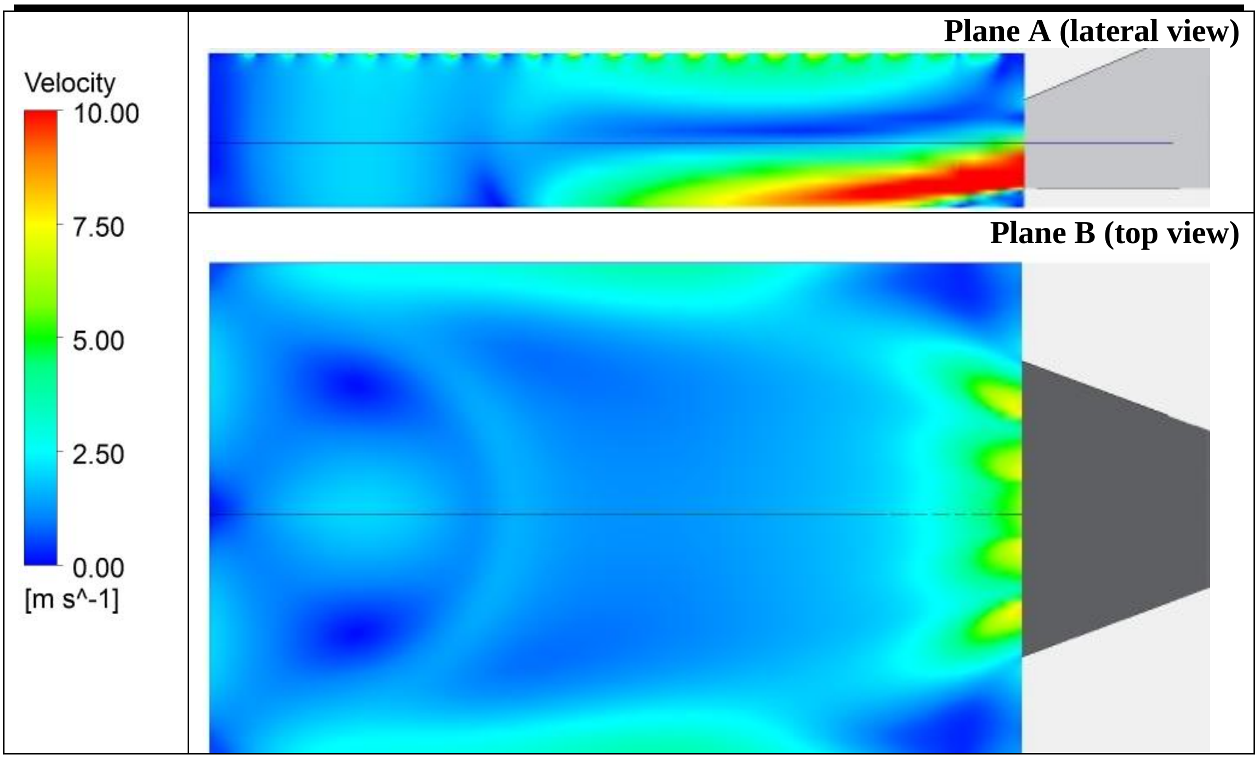

Fig. 18 Air compartment: velocity contours

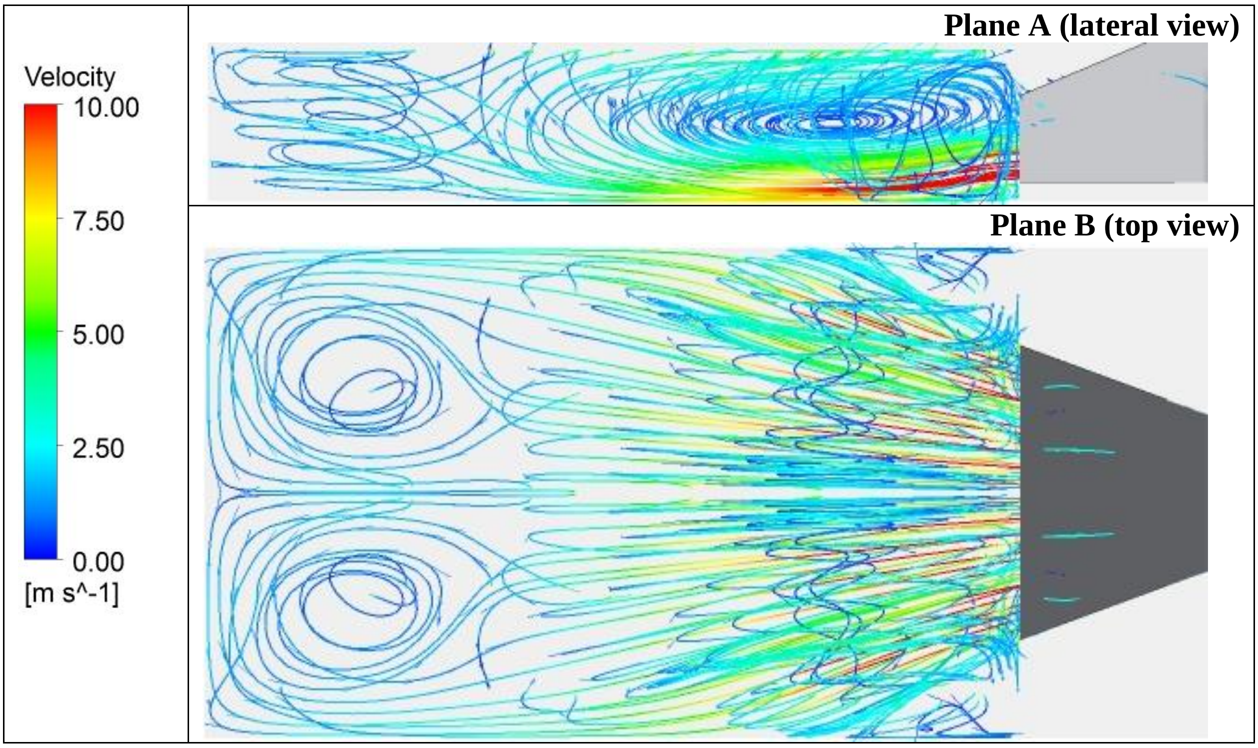

Fig. 19 Air compartment: streamlines

Growth chamber compartment

Fig. 20 and Fig. 21 illustrate the velocity field in the growth chamber. In order to show the velocity gradients, the velocity range of these figures was set between 0 and 1 [m/s]. The following observations can be made:

- High velocity values are reached at the back of the chamber where air is sucked into the cooling device. The mean velocity at the entrance of the cooler is 1.83 [m/s].
- Strong jet flows can be found between the perforated plate and the gullies. The details of a single jet flow are displayed in Fig. 21 section B.
- The presence of plants modelled with a localized pressure drop has a balancing effect on the flow field. Indeed it promotes a more homogeneous distribution of the air flow over the cross section when the air moves from the region in between the gullies to the one immediately above.
- The air velocity rapidly increases in the region outside the volume occupied by plants (90 cm from the lid of the gullies).

The behaviour of the velocity field seen in Fig. 20 is supported by the pressure field shown in Fig. 22. The mean value of pressure in the chamber is 19 [Pa]

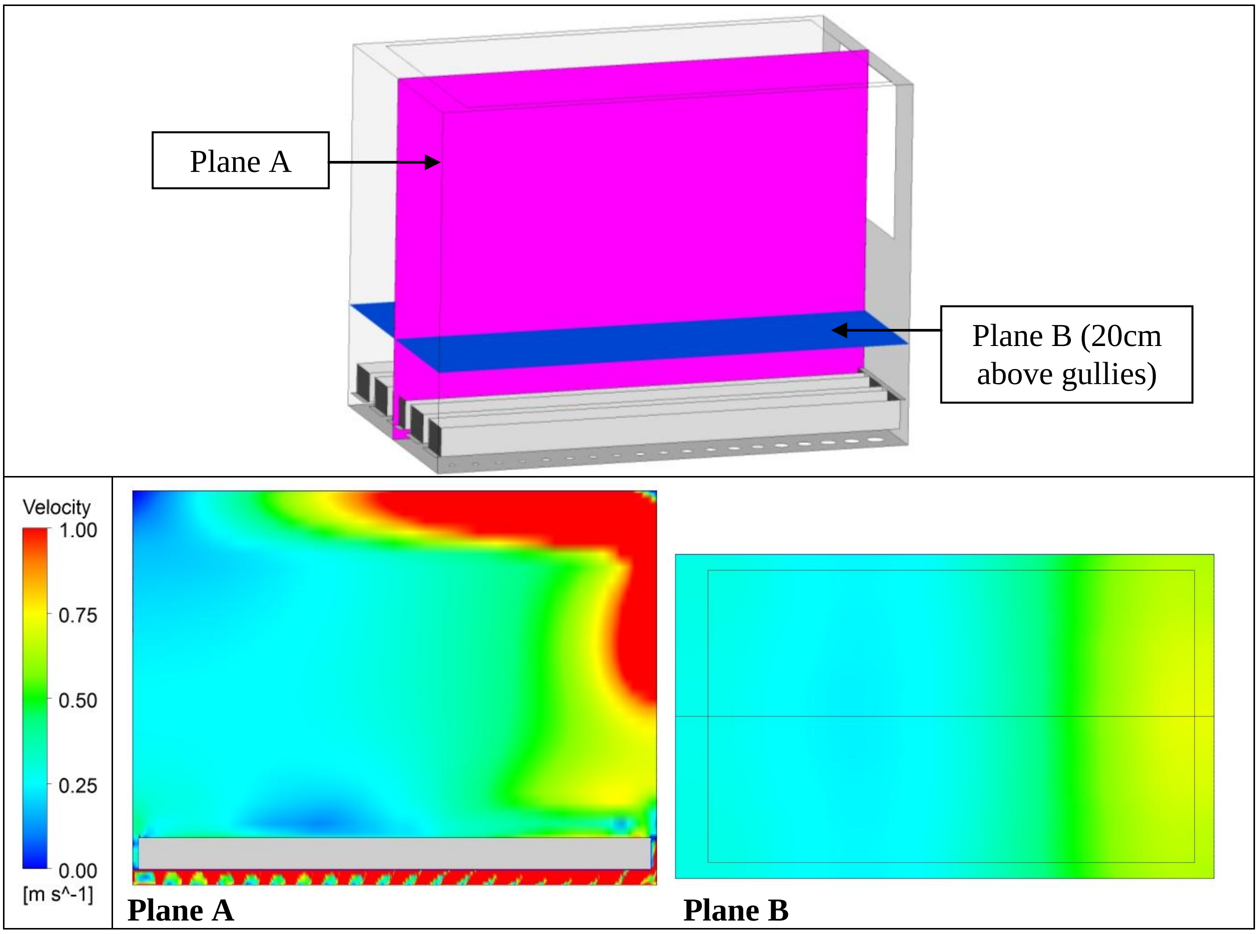

Fig. 20 Growth chamber: velocity

This document is confidential property of the MELiSSA partners and shall not be used, duplicated, modified or transmitted without their authorization
Memorandum of Understanding 19071/05/NL/CP

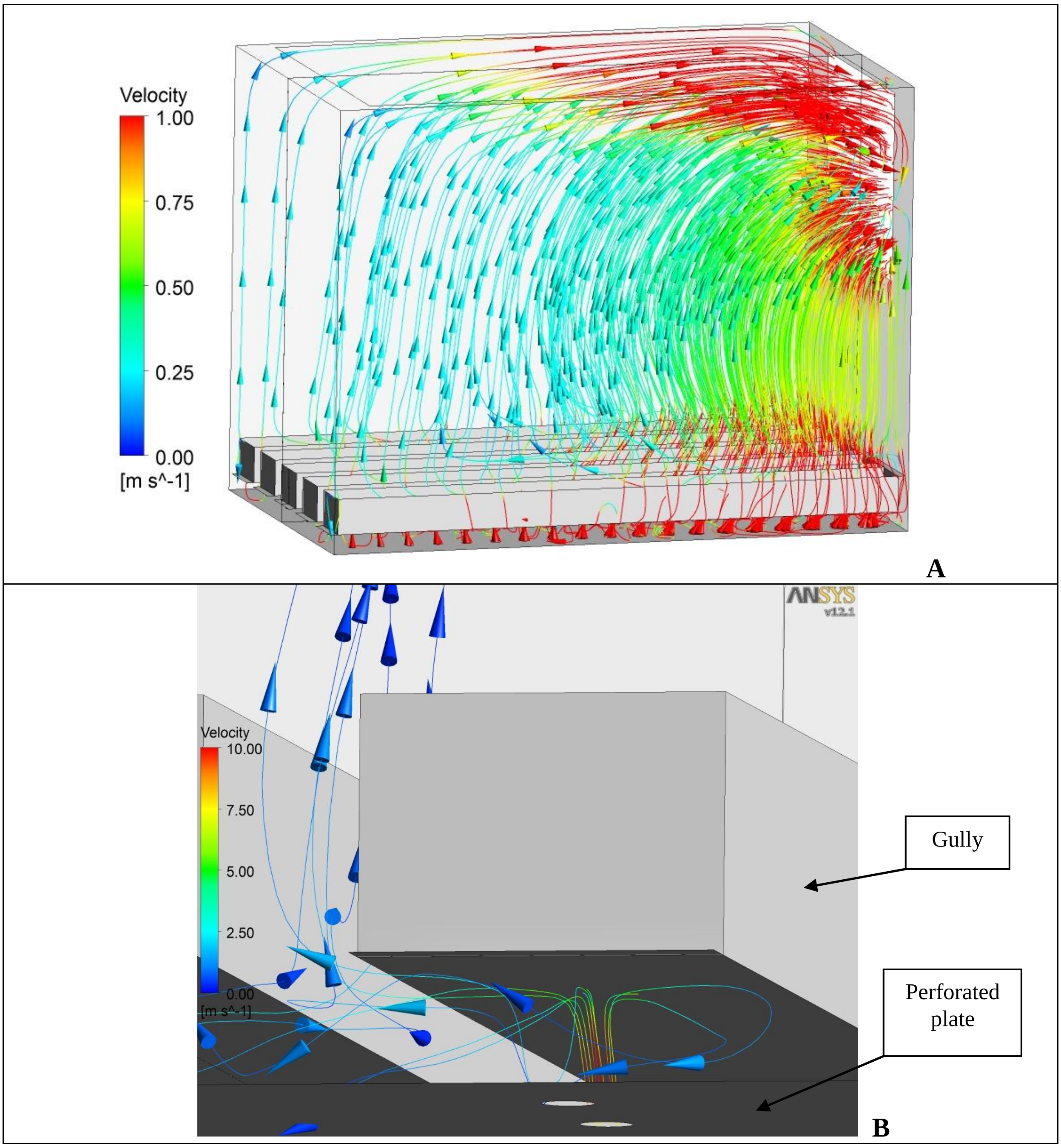

Fig. 21 Growth chamber: streamlines

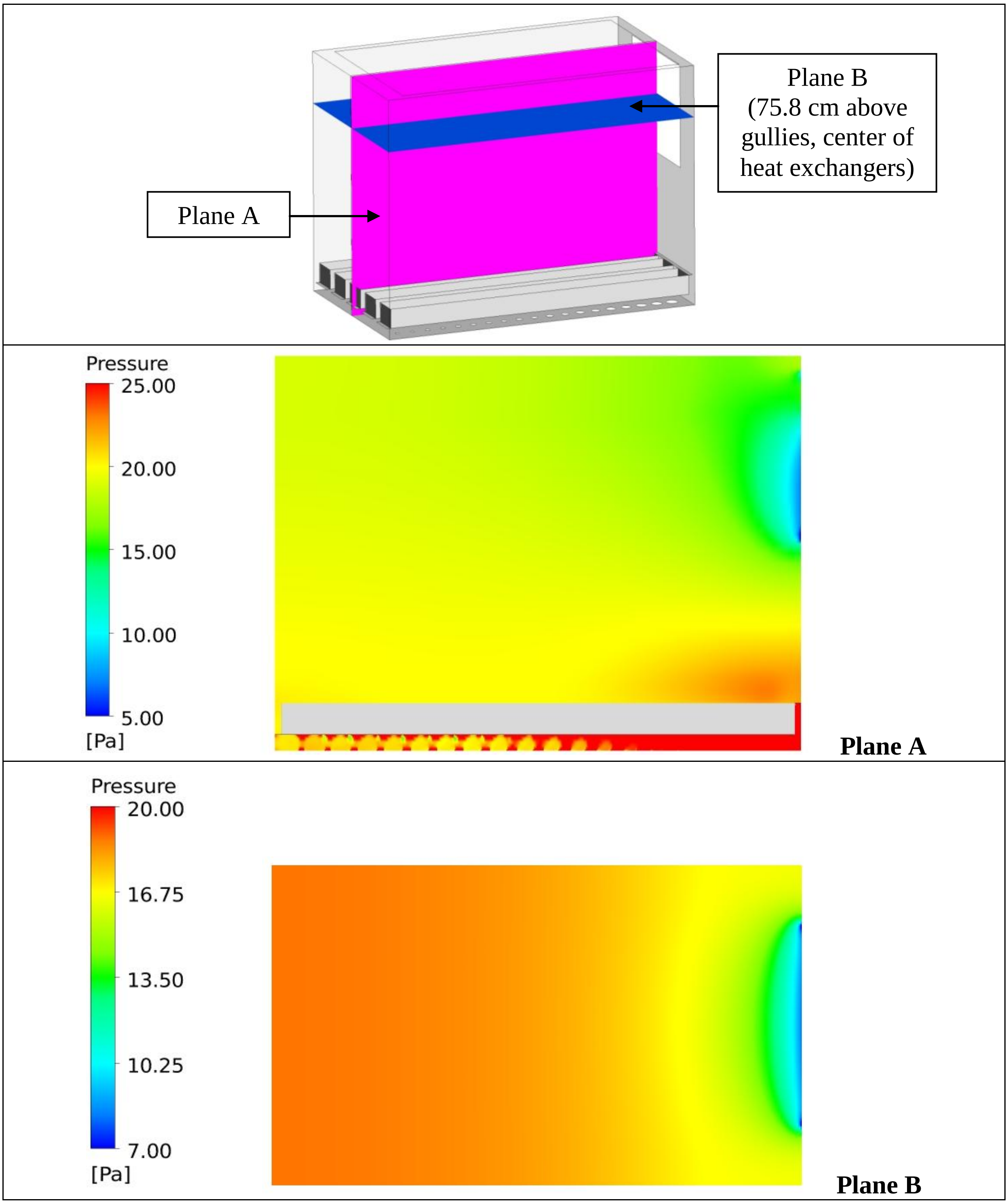

Fig. 22 Growth chamber: pressure

Perforated plate

In the following the fluid dynamic performance of the perforated plate is analysed. Tab. 5 shows the flow rate and the percentage of air flow for each row of holes. The location of the rows is displayed in Fig. 4.

Row	Flow rate [Kg/s]	Flow Distribution %
01	0,01316	1,77
02	0,01302	1,76
03	0,02007	2,71
04	0,02020	2,72
05	0,02903	3,92
06	0,02944	3,97
07	0,02942	3,97
08	0,02872	3,87
09	0,03770	5,09
10	0,03626	4,89
11	0,04489	6,06
12	0,04235	5,71
13	0,05012	6,76
14	0,04685	6,32
15	0,05437	7,33
16	0,05177	6,98
17	0,06076	8,20
18	0,06020	8,12
19	0,07301	9,85

Tab. 5 Perforated plate flow rates

Assuming that in the optimal scenario each row of holes is responsible of feeding 1/19 of air to the region immediately above, the target flow rate percentage for each row of holes should be 5,26%.

The row of holes from 1 to 10 are below the target while the opposite situation is observed from row 11 to row 19.

2.2 Conclusions

The CFD simulations carried out on the preliminary design of PCU air handling system allowed the investigation of its fluid dynamic performance.

The analysis of the results shows that:

- At the selected blower motor speed (Med Speed) the calculated flow rate is 0.74 Kg/s resp. 37141.27 l/min. This is approximately the upper limit of required flow rate as specified in TN 98.8.1. This will allow a broad range of flow rates as the blower flow rate can be controlled via a variable frequency drive. For the present case the selected blower is therefore sized correctly.
- At the simulated (high) flow rate strong jet flows are noticed at the level of the perforated plate. This will however not have any negative influence on plant growth as it is below the volume occupied by plants.
- The jet flow intensity is damped down by the presence of the gullies. 20 cm above the gullies (see Fig. 20) the air velocity is well below 1 m/s (see requirement SUB-CATM-FLO-2 to stay below 1 m/s at plant level). The distribution within the plane is still inhomogeneous (between 0.25 and 0.75 m/s).
- The flow field in the growth chamber is deeply influenced by two factors:
    - the design of the perforated plate which is not optimized. The air velocity gradient at gully level will be addressed in the following WP by proposing an optimized deign.
    - the strong suction action of the air outlet located at the back of chamber (mean velocity at the air outlet: 2 m/s).

The study herein presented will be further developed within WP8400 with the optimization of the design of the air handling system to address the inhomogeneity issues and the locally high flow rates described above. In addition a scenario with low flow conditions (blower flow rate reduced by half compared to the actual one) will be analysed. In this framework the thermal analysis of the growth chamber will also be performed for both the scenarios (high and low flow rates).

3 Oxygen Removal

Photosynthesis is a complex process that chlorophyllian plants carry out to assemble carbon-based molecules using CO_2 from the air (Fig. 23). CO_2 is added to a 5-carbons sugar, Ribulose-1,5-biphosphate (R-1,5-bP), to create two 3-carbons sugars: 3-Phospho-glycerate (3PG). This addition is known as a crucial step of the Calvin Cycle in photosynthesis. The enzyme responsible of this addition is the well-known RuBisCO.

But R-1,5-bP may also react with O_2 in a process called photorespiration. The O_2 is also added to R-1,5-bP by the RuBisCO, creating a competition between CO_2 and O_2 for the fixation. When the O_2 concentration is high, carbon fixation is inhibited: this process is known as the Warburg effect. Therefore, a high concentration of O_2 can lead to a decrease in the yield of photosynthesis at ambient concentrations of CO_2 (<400 ppm) in C3 plants. At higher levels of CO_2, the Warburg effect is suppressed even at elevated levels of oxygen.

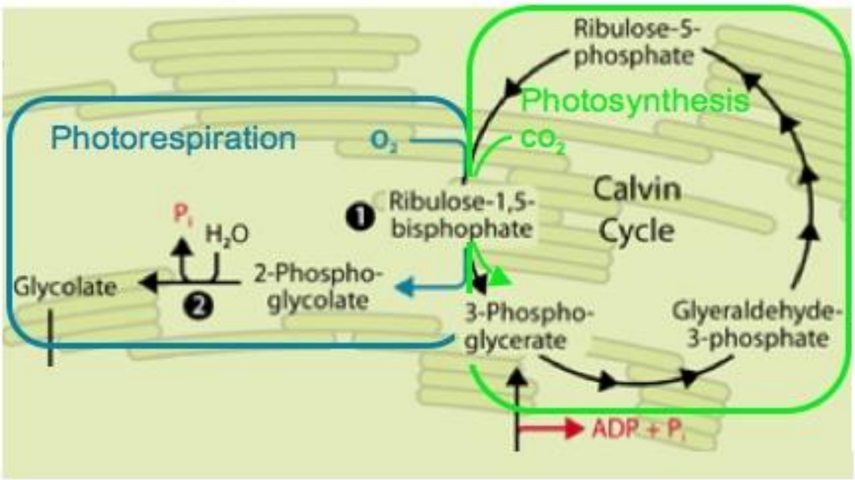

Fig. 23 Photosynthesis and photorespiration in the chloroplast

O_2 is a natural product of photosynthesis ($2n\ CO_2 + 2n\ H_2O + \text{photons} \rightarrow 2(CH_2O)_n + n\ O_2$) and is needed for crew survival. Consequently, the O_2 produced by the plants could simply be retrieved from the chamber in order to be used by the crew.

The volume of UoGuelph's growing chambers, also known as BlueBoxes, is 27 m^3, with a plant growing area of 5 m^2. At the time of the closure, the air within the chamber is composed of approximately 20% O_2 corresponding to 5,200 L of O_2.
During the first experiment on Avonlea where the largest increase in O_2 was observed, the maximum rate of O_2 production was 0.2% (54 L) per day (between 60 and 80 days after planting). In order to suppress the O_2 to an ambient level we therefore need to retrieve

minimally 54 L/d during the peak days. As the PCU three unit design is equal in growing area, a similar 54 L/d rate of removal would be the minimum required to offset O_2 production.

3.1 Oxygen combining reagents

Some molecules are known to bind O_2 efficiently in a reversible way: haemoglobin (Fe-based heme group) in animals, and many cobalt (Co-heme) based chelates. The chelates are recyclable as they can release O_2 afterwards, with an appropriate heating (170 C for 2 minutes) (Nishide et al, 1997). These methods are still being developed.

3.2 Using an O_2 concentrator to remove oxygen

The Pressure Swing Adsorption system (PSA)

O_2 deficiency causes stomach acid, bacterial, viral, parasitic infection, bronchial, chronic hostility and circulation problems. With age, some people become oxygen-deficient and need additional O_2 provision. A large industry of oxygen-concentrator companies invested in oxygen therapy and designed devices which retrieve oxygen from the air (20%) and concentrate it into a 95% O_2 flow for the patient to breath.

The main method to concentrate O_2 from air is named PSA, for Pressure Swing Adsorption. In this method, the nitrogen (N_2) and carbon dioxide (CO_2) are filtered by canisters composed of a zeolite molecular sieve. The enrichment of oxygen in air is due to the selective adsorption of nitrogen by interaction between N_2 and the molecular sieve. As air is being filtered through, nitrogen gas is adsorbed while oxygen (and argon) pass straight through. The zeolite is quickly saturated with nitrogen, so two zeolite beds are usually used together, one filtering air while the other is regenerated (Fig. 24 and Fig. 25).

This document is confidential property of the MELiSSA partners and shall not be used, duplicated, modified or transmitted without their authorization
Memorandum of Understanding 19071/05/NL/CP

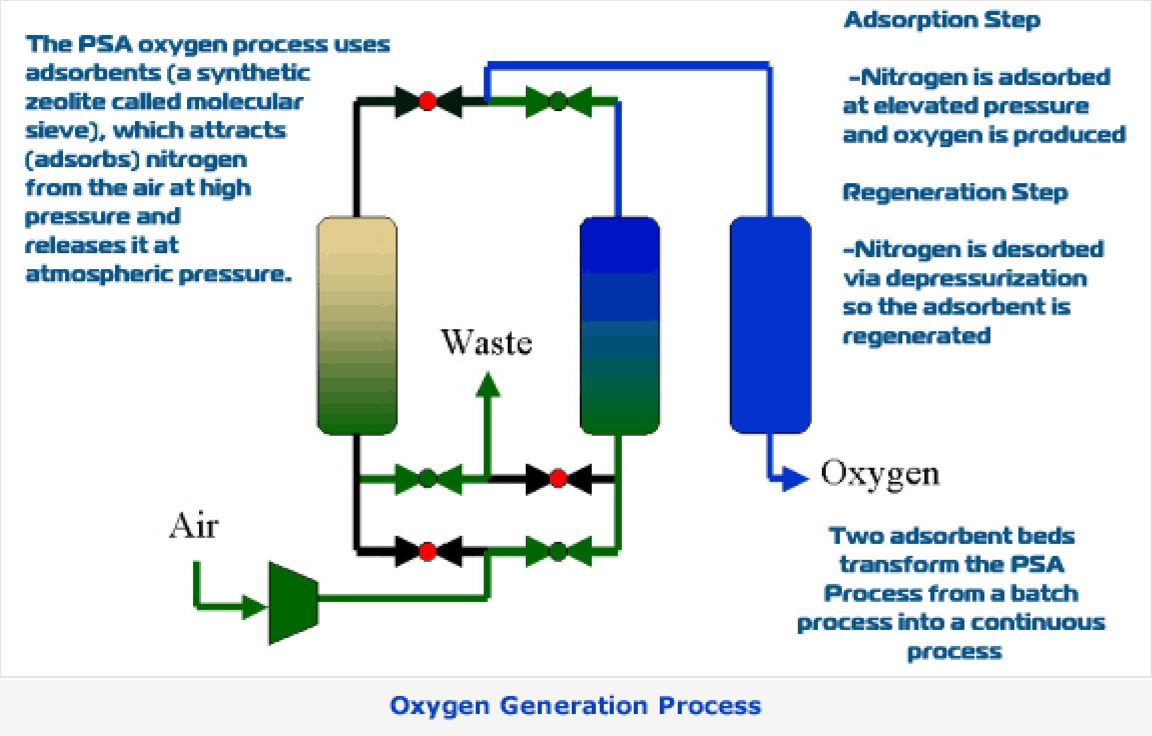

Fig. 24 Oxygen concentration process – pressure swing adsorption

The zeolites

The major components of an O_2 concentrator are the zeolite sieve beds. Zeolites are aluminosilicate minerals with complex crystal structures made with an open network structure of tunnels and cavities. The network structure gives an enormous surface area, which is largely inside of the solid. Moreover, because the molecules of only a certain size can make their way through the tunnels, the zeolites are highly selective. The selectivity of zeolites is also due to interactions between the ions of the crystal and the molecules passing through the crystal. Zeolties are already used for CO_2 scrubbing on International Space Station. Different types of molecular sieves exist, regarding their composition and properties. Papers report the use of zeolite 5A to filter O_2 specifically (as well as Argon).

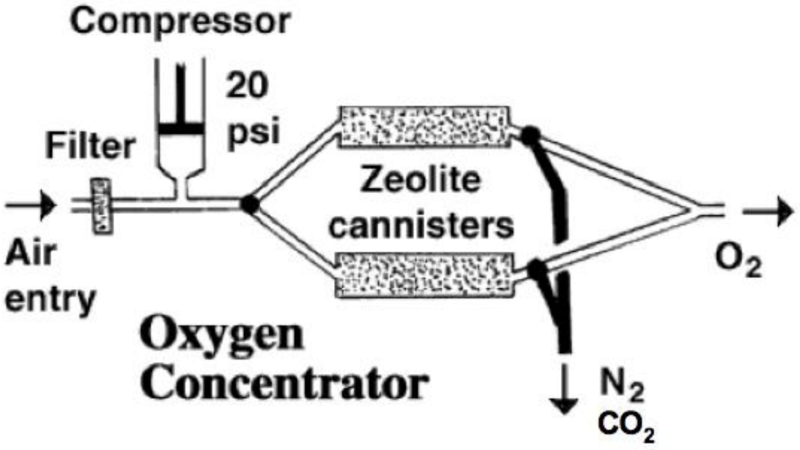

Fig. 25 Principle of two bed zeolite canister

The main problem with this method of oxygen removal is that the removal stream is not pure O_2. Nitrogen, carbon dioxide and water vapour, albeit in small amounts, will also be removed, making molecule balance calculations more difficult.

3.3 Removing O_2 while producing power: fuel cells

As the ground based growth chambers do not have to fit every requirement for space application, oxygen can be removed destructively and without the need for storage or further use. A fuel cell offers an ideal method for the selective removal of oxygen.

Description of a fuel cell

A fuel cell is a device in which a fuel is combined with oxygen to produce electricity, water, and heat. It operates much like a battery except that the reactants (and products) are not stored, but continuously fed to (and retrieve from) the cell.

A fuel cell works by catalysis: on the anode side, the component electrons and protons of the reactant fuel are separated. The protons are conducted through the membrane to the cathode, but the electrons are forced to travel in an external circuit (supplying power) because the membrane is electrically insulating, hence converting them to electrical power. On the cathode catalyst, oxygen molecules react with the electrons (which have travelled through the external circuit) and protons to form water. All fuel cells consist of two electrodes (anode and cathode) and an electrolyte (usually retained in a matrix) (Fig. 26).

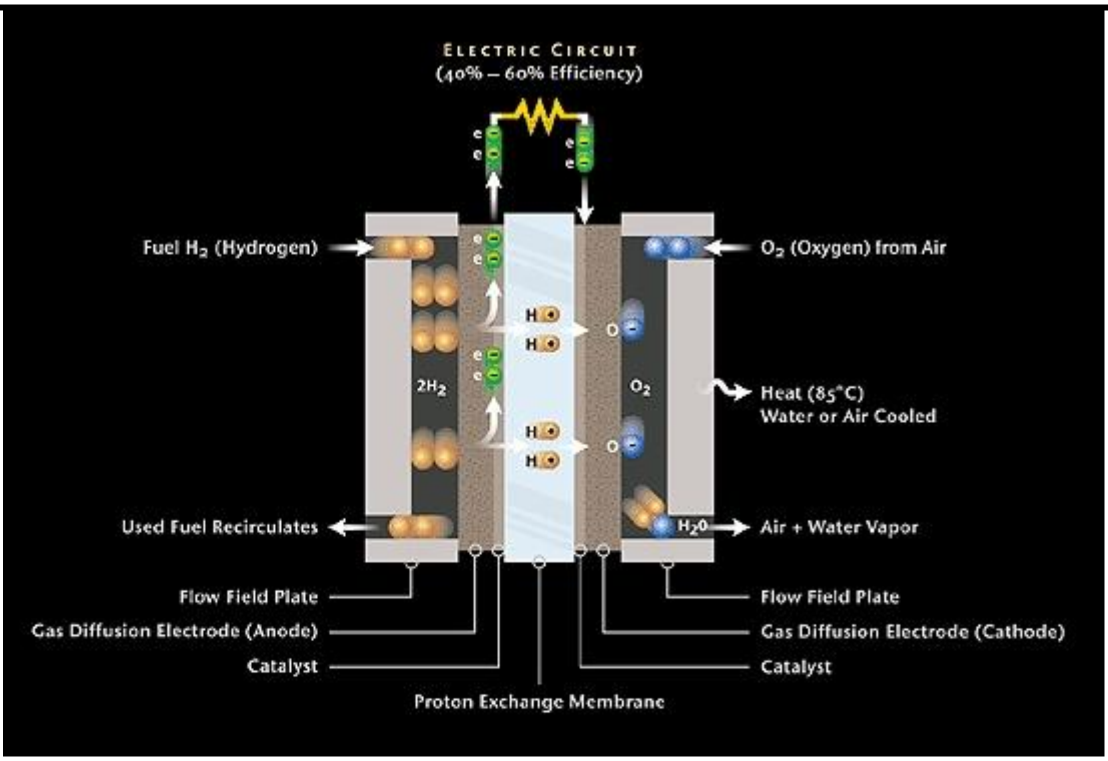

Fig. 26 Diagram of a hydrogen fuel cell

To function, the membrane must conduct hydrogen ions (protons) but not electrons as it would create a short-circuit in the fuel cell. The membrane must not allow either gas to pass to the other side of the cell, a problem known as gas crossover. Finally, the membrane must be resistant to the reducing environment at the cathode as well as the harsh oxidative environment at the anode.

Different forms of fuel cells are reviewed in the next section. Many combinations of fuels and oxidants are possible. A hydrogen fuel cell uses hydrogen as its fuel, and oxygen (usually from air) as its oxidant. Other fuels include hydrocarbons and alcohols. Other oxidants include chlorine and chlorine dioxide.

Types of fuel cells

Hydrogen Fuel Cells

The fuel used is hydrogen (H_2), composed of two protons and two electrons. In the archetypal hydrogen-oxygen proton exchange membrane fuel cell (PEMFC) design, a proton-conducting polymer membrane (the electrolyte) separates the anode and cathode sides. On the anode side, hydrogen diffuses to the anode catalyst where it later dissociates into protons and electrons. The only waste product is water, either liquid or vapour.

$$2\ H_2 = 4\ H+ + 4\ e^- \text{ (Anode equation)}$$
$$O_2 + 4\ H+ + 4\ e^- = 2\ H_2O \text{ (Cathode Reaction)}$$
$$2\ H_2 + O_2 = 2\ H_2O \text{ (Overall Reaction)}$$

Different electrolytes can be used, as described below.

Proton exchange membrane fuel cell (PEMFC)

The first PEMFC battery was created by General Electric for spacecraft Gemini in the early 1960s. The most commonly used membrane is Nafion by DuPont, which relies on liquid water humidification of the membrane to transport protons. This implies that it is not possible to use temperatures above 80 to 90C, since the membrane would dry out. Other, more recent membrane types, based on Polybenzimidazole (PBI) or phosphoric acid (see below), can reach up to 220C without using any water management.

Phosphoric acid fuel cell (PAFC)

Phosphoric acid fuel cells are a type of fuel cell that uses liquid phosphoric acid as an electrolyte. The electrodes are made of carbon paper coated with a finely-dispersed platinum catalyst, which make them expensive to manufacture. Phosphoric acid solidifies at a temperature of 40C, making startup difficult and restraining PAFCs to continuous operation. Major manufacturers of PAFC technology include UTC Power (also known as UTCFuel Cells), a unit of United Technologies, as well as HydroGen Corporation.

Alkaline fuel cell (AFC)

The AFC, also known as Bacon fuel cell after its British inventor, is one of the most developed fuel cell technologies and is the cell that flew Man to the Moon. NASA has used alkaline fuel cells since the mid-1960s in Apollo-series missions and on the Space Shuttle.

The two electrodes are separated by a porous matrix saturated with an aqueous alkaline solution, such as potassium hydroxide (KOH). Aqueous alkaline solutions do not reject carbon dioxide (CO_2) so the fuel cell can become "poisoned" through the conversion of KOH to potassium carbonate (K_2CO_3). Because of this, alkaline fuel cells typically operate on pure oxygen, or at least purified air. AFCs are the cheapest of fuel cells to manufacture. The catalyst required for the electrodes can be any of a number of different chemicals that are inexpensive compared to those required for other types of fuel cells.

Methanol Fuel Cells

This type of fuel cells relies upon the oxidation of methanol on a catalyst layer to form carbon dioxide (Fig. 27). Positive ions (H+) are transported across the proton exchange membrane to the cathode where they react with oxygen to produce water. Methanol is used as a fuel because it is naturally hydrogen dense (a hydrogen carrier) and can be steam reformed into hydrogen at low temperatures compared to other hydrocarbon fuels. Methanol and water react electrochemically at the anode to produce carbon dioxide, protons and electrons. The protons produced migrate through the polymer electrolyte to the cathode where they react with oxygen.

$$CH_3OH + H_2O = 6\,H^+ + 6\,e^- + CO_2 \text{ (Anode equation)}$$
$$O_2 + 6\,H^+ + 6\,e^- = 3\,H_2O \text{ (Cathode Reaction)}$$
$$CH_3OH + O_2 = 2\,H_2O + CO_2 \text{ (Overall Reaction)}$$

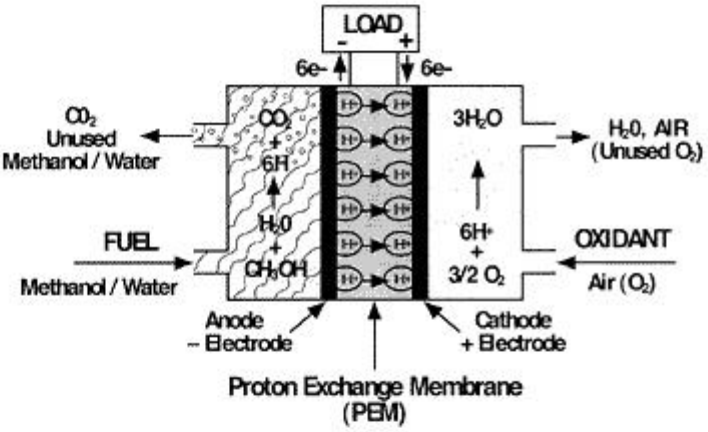

Fig. 27 Diagram of a methanol fuel cell

There are two types of methanol fuel cells:

Indirect Methanol Fuel Cells (IMFC)

Reformed Methanol Fuel Cell or Indirect Methanol Fuel Cell systems are a subcategory of proton-exchange fuel cells where methanol is reformed before being fed into the fuel cell. The fuel cartridge stores the methanol fuel, which is often diluted with up to 40% (by volume) water. The waste products with these types of fuel cells are carbon dioxide and water.

Direct methanol fuel cell (DMFC)

In contrast to indirect methanol fuel cells, where methanol is reacted to hydrogen by steam reforming, DMFCs use a methanol solution (usually around 1M) to carry the reactant into the cell; common operating temperatures are in the range 50 to 120C, where high temperatures are usually pressurized. DMFCs themselves are more efficient at high temperatures and pressures, but these conditions end up causing so many losses in the complete system that the advantage is lost; therefore, atmospheric-pressure configurations are preferred nowadays.

PCU Constraints

As we are in a sealed environment, the products of the reaction have to be taken into account. In both hydrogen and methanol fuel cells, the only products are water or CO_2, which are not a problem for growing plants. Methanol fuel cells are more difficult to find on the market for small applications. Alkaline fuel cells cannot be used in this application as they need pure oxygen or purified air to work properly. Phosphoric acid fuel cell can't work on a continuous basis, and take time to be turned on. The better choice would therefore be a **PEM fuel cell.**

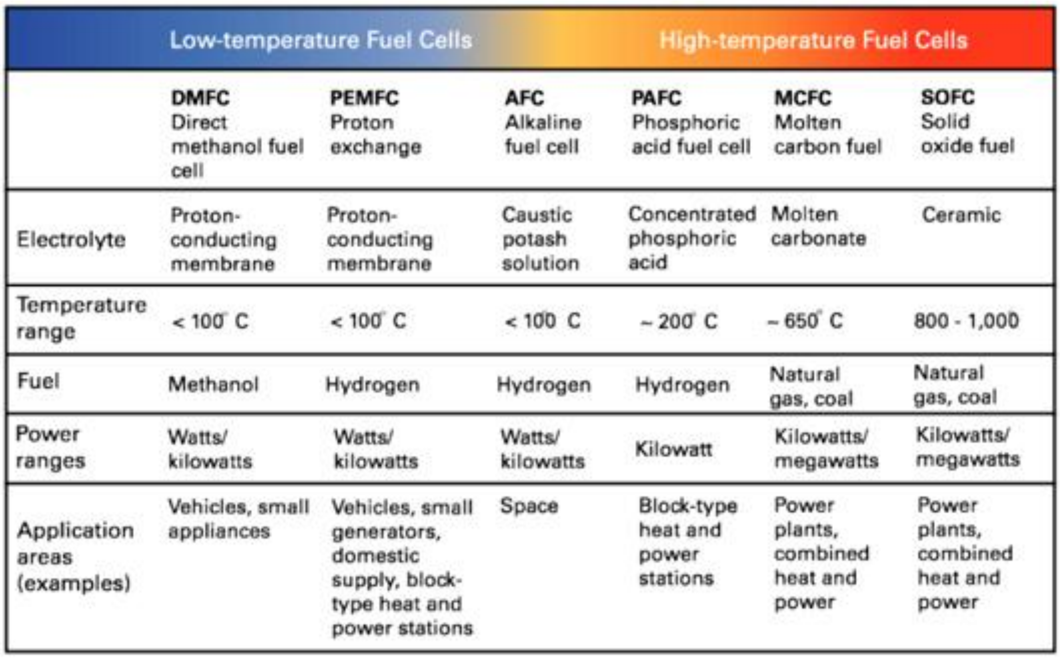

	Low-temperature Fuel Cells			High-temperature Fuel Cells		
	DMFC Direct methanol fuel cell	**PEMFC** Proton exchange	**AFC** Alkaline fuel cell	**PAFC** Phosphoric acid fuel cell	**MCFC** Molten carbon fuel	**SOFC** Solid oxide fuel
Electrolyte	Proton-conducting membrane	Proton-conducting membrane	Caustic potash solution	Concentrated phosphoric acid	Molten carbonate	Ceramic
Temperature range	< 100° C	< 100° C	< 100° C	~ 200° C	~ 650° C	800 - 1,000
Fuel	Methanol	Hydrogen	Hydrogen	Hydrogen	Natural gas, coal	Natural gas, coal
Power ranges	Watts/ kilowatts	Watts/ kilowatts	Watts/ kilowatts	Kilowatt	Kilowatts/ megawatts	Kilowatts/ megawatts
Application areas (examples)	Vehicles, small appliances	Vehicles, small generators, domestic supply, block-type heat and power stations	Space	Block-type heat and power stations	Power plants, combined heat and power	Power plants, combined heat and power

Fig. 28 Summary of different fuel cell types

Many different PEM fuel cells are available, and the pricing is mostly related to the amount of power generated by the fuel cell (Fig. 29). The consumption of H_2 and O_2 is increased as more power is produced.

To consume 54 L of O_2 per day, we would only need a **200 W fuel cell** (2.6 L/h = 62.4 L/D). A single fuel cell could be used and shared/cycled between the chambers, as continuous removal isn't required, or smaller units could be employed for each chamber. Power generated from the fuel cell would need to be dissipated or stored.

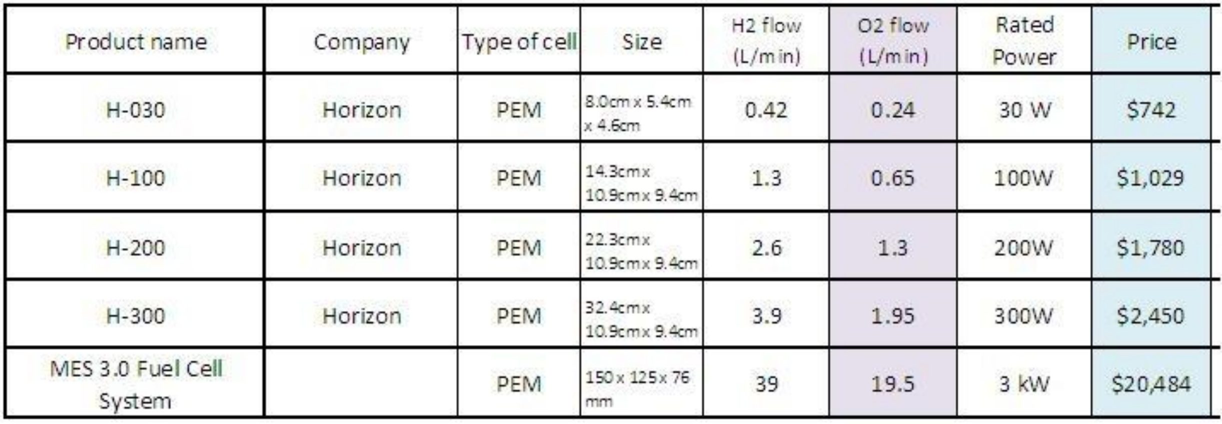

Product name	Company	Type of cell	Size	H2 flow (L/min)	O2 flow (L/min)	Rated Power	Price
H-030	Horizon	PEM	8.0cm x 5.4cm x 4.6cm	0.42	0.24	30 W	$742
H-100	Horizon	PEM	14.3cm x 10.9cm x 9.4cm	1.3	0.65	100W	$1,029
H-200	Horizon	PEM	22.3cm x 10.9cm x 9.4cm	2.6	1.3	200W	$1,780
H-300	Horizon	PEM	32.4cm x 10.9cm x 9.4cm	3.9	1.95	300W	$2,450
MES 3.0 Fuel Cell System		PEM	150 x 125 x 76 mm	39	19.5	3 kW	$20,484

Fig. 29 Pricing from www.fuelcellstore.com

3.4 Conclusions

There are numerous methods of removing oxygen from the atmosphere. Ultimately the major oxygen consumer in a space/Mars/Moon scenario will be the astronauts, but during testing of plant performance prior to ALS development, oxygen must be removed selectively without the aid of human respiration. For the purposes of oxygen removal from a plant environment, the hydrogen fuel cell is the best candidate as it selectively reacts with oxygen to produce water. Other methods can have unwanted by-products or are cross reacting with other atmospheric constituents. As oxygen is constantly monitored, the amount of water added by the fuel cell can be calculated directly from oxygen depletion, or measured directly through condensation and collection.

4 Ethylene Mitigation

Ethylene is produced from essentially all parts of higher plants, including leaves, stems, roots, flowers, fruits, tubers, and seedlings. Ethylene production also plays an important role in regulating many plant processes, ranging from germination to senescence. Its presence in high concentrations can lower yield in all candidate ALS crops, and should therefore be removed from the growing area.

4.1 Inhibiting the ethylene effects on plants

In order to avoid the effect of ethylene on plants, it is possible to inhibit the ethylene receptors buy using a competitor, the **1-MCP** (1-methylcyclopropene, C_4H_6). 1-MCP has been approved for fruits and vegetable applications and is generally spread after harvest or during storage and transportation. But the use of a chemical inside a closed environment should be avoided because its degradation products can be toxic for both humans and plants.

This document is confidential property of the MELiSSA partners and shall not be used, duplicated, modified or transmitted without their authorization
Memorandum of Understanding 19071/05/NL/CP

4.2 Natural degradation of Ethylene using biofilters

Some bacteria can use ethylene as a source of carbon. It is the case for some bacteria from the Pseudomonas family, like *P.putida* and *P.fluorescens*. These bacteria are gram negative, aerobic and do not form spores. When grown on an activated carbon media, they can achieve almost complete removal (98%) of ethylene within 24 hours.

The metabolism of ethylene by bacteria produces CO_2 (1000 mg.m^3 within 90 days). As the plants can re-use this CO_2, Pseudomonas could be used in bio-filters to remove ethylene from closed growth chamber. No experiments have been conducted so far.

Pseudomonas have other beneficial aspects that are of great interest when looking at plant growing efficiency. It has been shown that wheat inoculated with *P.fluorescens* had a greater biomass and a greater seed mass than the control without inoculation (Shaharoona et al, 2008). The addition of bacteria to the growing system to provide enhanced growth and ethylene reduction should be investigated. A major disadvantage of this method to reduce ethylene production is that it will be difficult to control ethylene production such that the ethylene levels needed for normal vegetative growth, flowering and fruit development can be maintained. The possibilities mentioned below offer good alternatives.

4.3 Ethylene removal by the food industry

The food industry is concerned the ethylene involved in ripening, especially during transportation of fruits and vegetables. A wide number of technologies now exist to reduce the ethylene percentage in air in closed environments.

- Ethylene removal stickers

A brand new technology appeared on the market in February 2009. Stickers designed by *IT's Fresh*! are designed to absorb ethylene while being safe for food production. The same concept exists in sachets.

- Air filtration systems

A large range of very effective air filtration systems are now on the market, using different technologies to purify air from ethylene. The filters have to be replaced often and are usually based on metallic oxides or KMnO4.

4.4 Ethylene removal using zeolites

Zeolite 5A can bind ethylene, N_2 and CO_2, therefore it can’t be used to selectively remove ethylene in a plant growing system because it would remove CO_2 and N_2 and the same time.

This document is confidential property of the MELiSSA partners and shall not be used, duplicated, modified or transmitted without their authorization
Memorandum of Understanding 19071/05/NL/CP

Further investigation should be conducted to determine if zeolite could be used in growing chambers.

4.5 Chemical degradation of ethylene

Ethylene (or ethene in the IUPAC nomenclature) is an alkene (it possesses a double bond), and its formula is C_2H_4 or $H_2C{=}CH_2$. The most characteristic chemical reaction of an alkene is an addition reaction, in which atoms supplied by the other reactant are attached to the atoms joined by the double bond

Numerous ways of degrading ethylene exist: hydrogenation, combustion, oxidation, hydration, polymerization, and ozonolysis. All those chemical reactions produce by-products that are more or less toxic or useless in a plant growing system.

We will here focus on the **ozonolysis** of ethylene, since its by-products are the less toxic and because ozone is already used on the Space Station.

Ozonolysis cleaves an alkene to carbonyl compounds

$$CH_2CH_2 + O_3 = 2\ H_2CO \text{ (Formaldehyde)}$$

Formaldehyde can be easily removed by the plants themselves and ozone can be produced from O_2, itself produced by plants using CO_2.

The ozonolysis is a well studied chemical reaction, and several improvements in yield and safety have been made in the last part of the 20th century. The theoretical reaction between O_3 and ethylene leads to the production of a dangerous ozonide. In order to avoid the formation of this compound, O_3 is mixed with O_2-containing gas, usually air. In addition, O_2 inhibits the rate of disappearance of O_3 in the reaction with alkenes.

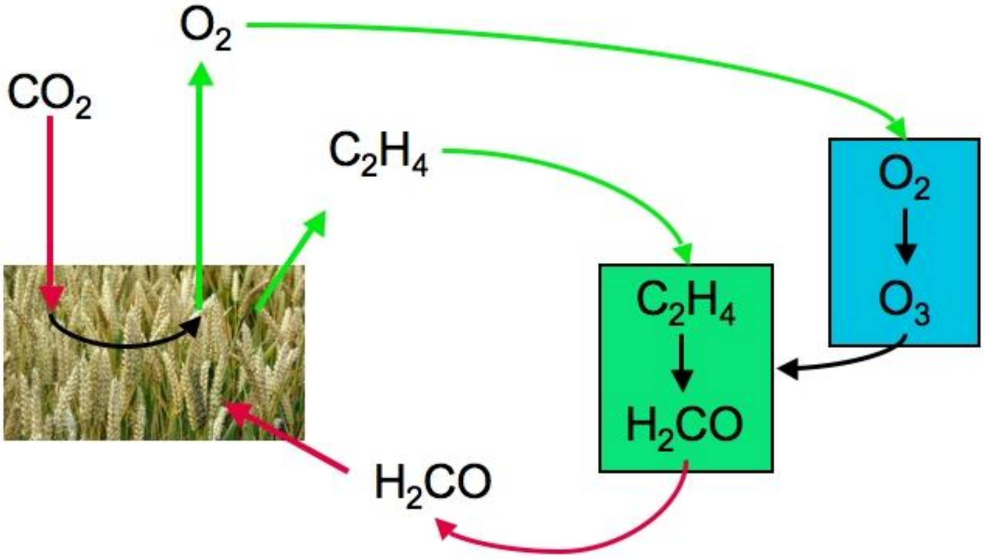

Fig. 30 Integration of all reactions for the ozonolysis of ethylene

In this procedure, a catalyst is also needed to perform the ozonolysis. Some researchers recommend the use of silver. Aluminum oxide or Carborundum (known as well as silicon carbide, SiC) can be mixed with silver oxide (15% to 35% by weight of silver). Using the air as a source of oxygen, the resultant oxygen-and-ozone-containing gas must mix with the ethylene only in the presence of the catalyst. The reaction is carried out at a temperature from 220 C to 300 C under atmospheric pressure.

4.6 Conclusions

There is no definitive method for the removal of ethylene from a plant environment. Research should be engaged to elucidate a method that provides adequate selective removal, but in the interim, simplified methods that combine daily ethylene evaluation (gas chromatography) with removal using $KMnO_4$ substrates should be employed in the PCU.

5 References

Addison M. Rosenkrans and Alvin I. Krasna, 2004. Stimulation of hydrogen photoproduction in algae by removal of oxygen by reagents that combine reversibly with oxygen, Biotechnology and Bioengineering, 26(11):1334 – 1342

Chaerle L., and Van der Straeten D., 2008. Proposal for MELLiSSA Food Characterisation Phase 1

Darlington A, et al., The use of biofilters to improve indoor air quality: the removal of toluene, TCE, and formaldehyde, Department of Horticultural Science, University of Guelph, Canada

Gi-Moon Nam et al., 2005. Equilibrium Isotherms of CH4, C2H6, C2H4, N2, and H2 on Zeolite 5A Using a Static Volumetric Method, J. Chem. Eng. Data. 50: 72-76

Jones L. and Atkins P., 1999. Chemistry: Molecules, Matter and Change, 4th ed, ISBN 0-7167-3254-8

Kim et al.. 2006. Assessment of ethylene removal with Pseudomonas strains. J. Hazard Mater. 131 (1-3): 131-6

Moon et al, 1986. Air separation by adsorption on molecular sieve 5A., Korean J. of Chem. Eng. 3(1):15-21

Nishide et al. 1997. An oxygen-releasing device: reversible oxygen release from a cobalt chelate-carbon composite in response to applied voltage. J. Mater. Chem. 7(10):2151-2153

Shang Fa Yang and Neil E. Hoffman. 1984. Ethylene biosynthesis and its regulation in higher plants, Ann. Rev. Plant Physiol. 35:155-89

Shaharoona et al., 2008. Fertilizer-dependent efficiency of Pseudomonads for improving growth, yield, and nutrient use efficiency of wheat (Triticum aestivum L.). Appl Microbiol Biotechnol 79 (1):147-55

Story et al., Method of reductive ozonolysis of olefins to produce carbonyl compounds and intermediate products, June, 1992, US Patent

Technical Note 98.4.21: Crop cultivar test results. UGent (2010). *Food Characterization One.* Gent

Technical Note 98.7: Definitions of PCU requirements. UGent (2010). *Food Characterization One.* Gent

Technical Note 98.8.1: PCU Specifications. UGent (2010). *Food Characterization One.* Gent

V. S. Bagotzky, et al., Fuel Cells: State-of-the-Art and Major Scientific and Engineering Problems, Russian J. of Electrochemistry, Vol. 39, No. 9, 2003, pp. 919–934. Translated from Elektrokhimiya, Vol. 39, No. 9, 2003, pp. 1027–1045.

Internet ressources:

http: //www.epa.gov/pesticides/biopesticides/ingredients/factsheets/factsheet224459:html

This document is confidential property of the MELiSSA partners and shall not be used, duplicated, modified or transmitted without their authorization
Memorandum of Understanding 19071/05/NL/CP